International Journal of Multidisciplinary Studies and Innovative Research

ISSN: 2737-7172 (O), ISSN: 2737-7180 (P)
Volume 11, Number 03, pp. 1530-1560
DOI: 10.53075/ljmsirq/45435745353533

Prospective Small Hydroelectric Power Sites along the Black Volta River

Salifu Ali Dayinday
Catholic University of Ghana, Fiapre-Sunyani
E-mail: dayindayali@gmail.com

How to Cite: Salifu Ali Dayinday (2023). Prospective Small Hydroelectric Power Sites along the Black Volta River. *International Journal of Multidisciplinary Studies and Innovative Research,* 11(3), 1530-1559.

Abstract: This study investigates the potential sites for Small Hydroelectric Power (SHP) generation along the course of the Black Volta River. The growing demand for clean and sustainable energy sources has led to renewed interest in harnessing hydropower resources. The objective of this research is to identify and assess suitable locations for SHP development, taking into consideration factors such as river morphology, flow characteristics, topography, and environmental impacts. By employing a systematic approach and utilizing geospatial analysis, the study aims to contribute valuable insights into the feasibility and viability of implementing SHP projects within this region. The outcomes of this research could provide a foundation for future decision-making processes regarding the sustainable utilization of hydroelectric potential along the Black Volta River while minimizing ecological and social implications.

Keywords: Power, Black Volta River, Hydropower Generation, Sustainable Energy, Geospatial Analysis, Feasibility Assessment, Environmental Impact, Renewable Energy, River Morphology

1. INTRODUCTION

The Fifth Assessment Report of the Intergovernmental Panel on Climate Change (IPCC) concluded that "Warming of the climate system is unequivocal, and since the 1950s, many of the observed changes are unprecedented over decades to millennia" (IPCC, 2013b). There is a need now to consider the likely positive and negative impacts of climate change on the natural environment and people across the globe. Deltas are widely recognized as being highly vulnerable to the impacts of climate change particularly sea level rises and river runoff changes (Hoang et al., 2016; Kay et al., 2015; Nepal and Shrestha, 2015; Nicholls et al., 2016; Smajgl et al., 2015; Whitehead et al., 2015b). Many are also impacted by the effects of urbanization and changes in sediment input (Allison et al., 2017; Gu et al., 2011; Syvitski et al., 2005). Low and mid latitude deltas have some of the highest population densities in the world; with more than 500 million, often poor, residents living in deltas globally (Ericson et al., 2006). Therefore, it is essential to develop methods to assess the vulnerability of deltaic areas and establish adaptive strategies including migration available to deltas residents. To do so, a set of physical, geographical and chemical models are needed to simulate the catchments and the river systems that go into the delta estuary. The simulations from the catchment models could be provided to

the downstream coastal modelers in order to assess impacts of climate change on the delta estuary and coastal systems.

As the scientific consensus concerning climate change, and awareness of the impacts on river systems has increased in recent years, there is a growing need to incorporate climate change into water resources management and water storage planning for large catchments (Sadoff and Muller, 2009). However, across much of sub-Saharan Africa, climate change is given low priority. In many countries there has been few systematic evaluation of changing river flow regimes and the potential influence to the coastal zone under climate change and it is given little consideration in the planning of future water resources development. As part of the DECCMA project (Hill et al., 2018), the focus of this work is Volta delta in Ghana, Africa, in particular Volta River system.

The Volta River system is a transboundary catchment and the principal water source for approximately 24 million people in six riparian states, namely Ghana, Burkina Faso, Benin, Cote d'Ivoire, Mali and Togo (McCartney et al., 2012). The catchment drains into Lake Volta in Ghana, the largest man-made lake in the world, and a major supplier of hydropower to Ghana. The catchment is primarily agricultural providing food supplies to rural and urban areas, demonstrating the classic water, food, energy nexus. The basin's population is projected to nearly double in number from 19 million in 2000 to 31 million in 2025 and 32 million in 2050 (McCartney et al., 2012). Water resources in the Volta Basin have been under increasing pressure in recent years as significant population growth and economic development in Ghana and Burkina Faso has resulted in larger abstractions to meet increasing demand (Van de Giesen et al., 2001).

Several studies in the past indicated a reduction in rainfall and runoff in the Volta Basin since the 1970s (Gyau-Boakye and Tumbulto, 2000; Lacombe et al., 2012; Owusu et al., 2008), as well as an increase in drought frequency (Kasei et al., 2010). This may be attributable to changing climate. There is an agreement between different climate models that the climate of Volta Basin will warm over the course of the 21st century, though the magnitude of the warming differs between different models and different scenarios for future greenhouse forcing of the global climate system (IPCC, 2013a). It is uncertainty between models in the sign of future rainfall changes in the basin that is more likely to complicate the management of the basin's water resources. For example, McCartney et al., 2012 used a dynamic regional climate model (CCLM), a hydrological model (SWAT) and a water resource model (WEAP) to assess a "middle impact" (between extremes) climate change scenario on existing water uses within the basin (McCartney et al., 2012). This work suggested that annual average rainfall, runoff and mean groundwater recharge will decrease by 2050. In contrast, Awotwi et al. (2015) (Awotwi et al., 2015) used an ensemble of the Regional Climate Model (REMO) and suggested that the White Volta sub-basin will experience 8% precipitation increase with a 26% increase in surface runoff. The disagreement between these studies largely reflects the inconsistency in projecting rainfall from different climate models/scenarios.

2. MATERIAL AND METHODS

Profile of Study Area

The Black Volta River (Mouhoun) originates from the Kong Mountains situated in the Dinderesso Forest Reserve in southwestern Burkina Faso, and passes through Ghana, Burkina Faso, Mali, and Côte d'Ivoire (shown in figure 6). The river serves as a natural boundary between Ghana and Burkina Faso, and later between Ghana and Côte d'Ivoire, as it moves southward. It covers a small area in western Ghana, extending to the border with Ivory Coast. The total area drained by the river is 142,056 km2, with Ghana contributing 33,302 km2, Ivory Coast 12,836 km2, Mali 8,710 km2, and Burkina Faso 87,208 km2. The Sourou, Benchi, Chuko, Laboni, Gbalon, Pale, Kamba, and Tain are significant tributaries to the Black Volta. The Sourou originates in Mali and joins the Mouhoun where the latter changes its direction from north to south. The flow of Mouhoun is regulated by the Sourou depression, which temporarily traps its waters during high discharge, and replenishes the Mouhoun during low water levels. The Lery Dam plays a critical role in regulating the river's flow. The gradient of the river is steeper in the upper reaches, leading to a higher flow, while it becomes less steep in the valley, causing slower water flow and infiltration into the ground (e.g., at Boromo hydropower station). Before the construction of the Lery Dam, the river flowed toward Mali during the rainy season. The low flow in

Boromo may be due to water abstraction upstream at Tenado. The average annual volume of the river is 7.673 x 106 m3year-1 (MWH 1998a). The mean inflow into Ghana is determined using discharge measurements at Lawra, which is 34.75 m3s-1 during the dry season and 373.79 m3s-1 during the wet season.

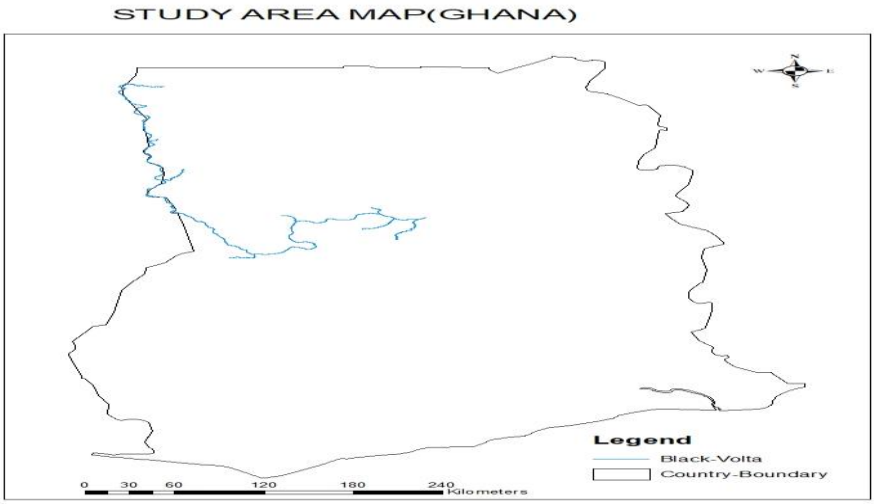

Figure 1: Study area (Ghana)

Model

The study used the Digital Elevation Model 30m by 30m resolution from USGS, Precipitation data at rain gauge data from NOAA and Ghana Metrological Agency, Boundary shape file from Ghana Institute of Survey, Global soil data from FOA, and Global land use from USGS. Also used data Landsat data. The study made use of ArcGIS computer software for processing and analysis.

Data Preparation

Digital elevation model data was downloaded from USGS and imported into the ArcGIS software. The data was projected into UTM Zone 30N and merged. The boundary shape for the study area was used to extract the various elevation for the study area. For the rainfall data, monthly rainfall data was collected from five rain gauge stations in the study area to calibrate the global rain gauge data download from NOAA. IDW tool in ArcGIS was used to interpolate the data to create a raster surface. The land sat data was downloaded from USGS and imported into ArcGIS. The data was projected to UTM zone 30 N and pan-sharpened into 15m-by-15m resolution, The various tiles were merged and the extract by mask was done to identify the region of interest using the study boundary shape file. Similarly, for the global soil data, the clip tool was used to clip regions of interest. The various soil was enabled using symbology. The data was then converted into raster format using polygon to raster tool. The raster data was then projected into UTM Zone 30 N.

Land Use Land Cover Analysis

This analysis helps to better understand the present and historical land use land cover (LULC) of the basin which will in turn affect the runoff generated in the different years. LULC also serves as a guide in the final selection of proposed sites for SHP development.

Data Acquisition and Pre-processing for LULC Analysis

Two (2) Landsat images were used to aid in the assessment of LULC analysis in the Black Volta Basin. The Landsat 7 ETM+ images were downloaded from the United States Geological Survey's (USGS) website (Table 1).

A geometric correction was done on each Landsat image using the Semi-Automatic Classification Plugin for Pre-processing plugin of Landsat images in the QGIS interface. Image enhancement was then performed to improve the

visual representation of the data. The relevant bands were composited and mosaicked to achieve one image. The Black Volta basin was clipped on the mosaicked image.

Image Classification and Validation

Unsupervised classification was carried out to give an idea of the existing land uses in the area as the site had not yet been visited. Four dominant classes were identified and their pixel values matched for each dominant class.

Post Classification

The accuracies of the classified image were determined by the application of statistical analysis for validation. Overall accuracy, producer's accuracy, and user's accuracy were all determined based on the confusion matrix. Information on the correct and incorrect predictions of classification is provided in a confusion matrix. This is done by comparing the classified map and the ground data. The image was validated using data obtained from aerial images. The error matrix is constructed as shown in Table 1

Table 1: Error matrix for accuracy assessment

		Reference Map				
		Class 1	Class 2	Class 3	Class 4	Row Total
Classification	Class 1	N_{11}	N_{12}	N_{13}	N_{14}	N_1
	Class 2	N_{21}	N_{22}	N_{23}	N_{24}	N_2
	Class 3	N_{31}	N_{32}	N_{33}	N_{34}	N_3
	Class 4	N_{41}	N_{42}	N_{43}	N_{44}	N_4
	Column Total	M_1	M_2	M_3	M_4	N

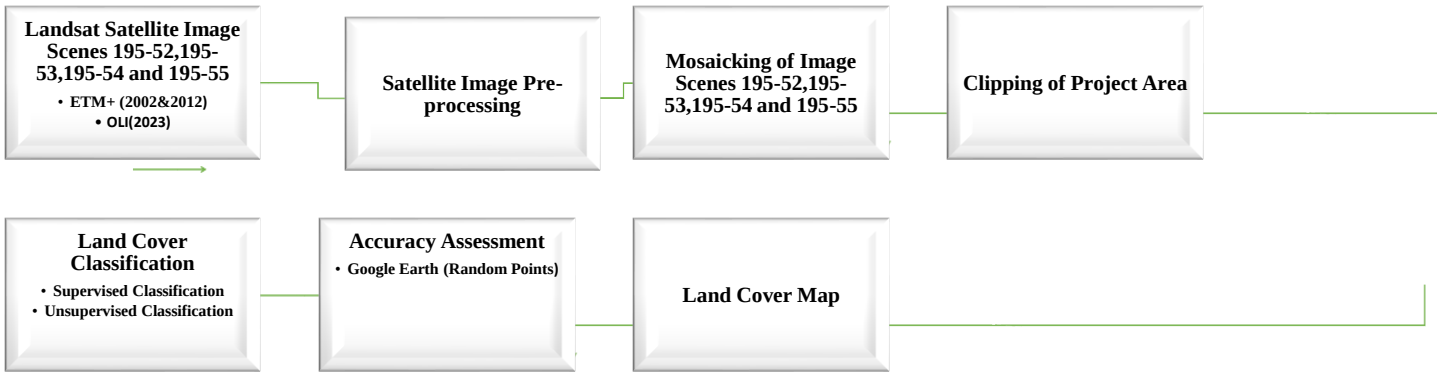

Figure 2: Flow chart for land use land cover analysis

Siting of Potential SHP Sites

Data Acquisition

Digital Elevation Models (DEM) were obtained from the United States Geological Survey's (USGS) website. These data have a grid size of 30mx30m. The DEM was used to develop the flow direction, flow accumulation, and the river network. The DEM is ultimately used to determine the available head at different locations.

DEM Pre-processing

The DEM provided information on the elevation in the area. It is a base map from which several thematic maps can be developed in a GIS environment. The pre-processing began with the filling of sinks; sinks occur due to errors in the resolution of data or the rounding of this elevation to the nearest integer value. The direction of the flow was also determined; this tool determines the direction of flow from each cell in the raster. The flow is then accumulated; cells draining into each downstream cell. The stream network is generated from the flow accumulation map.

Preliminary Potential Hydropower Sites

The generation of hydropower is a function of the amount of flow and the head available. With this preamble as the basis, the selection of an appropriate head depended on some criteria, some of which were adopted from (Popat & Tarrant, 2023) and (Rafee et al., 2019).

The location of potential sites based on a suitable head is dependent on the amount of flow. The order of the stream gives an idea of the amount of flow available. A higher-order stream indicates the probability that more water flows within that stream. (Idrissou et al., 2020)The different systems of ordering streams are the Strahler stream order, Classic stream order also known as Hack's stream order, Shreve stream order, and the Horton stream order and other systems. The Strahler was used because of its simplicity and the wide use of the method across the globe to order stream networks (Barnieh et al., 2020). Therefore, to ensure that the flow will be sufficient, streams of order 3 and above were used.

Strahler's method of stream ordering was used in the ArcGIS environment. This method assigns the order based on the stream network. The origin of the stream is classified as 1st order, and the stream generated by the confluence of two first-order streams is classified as 2nd order. (Gebrechorkos et al., 2023)The confluence of two (2) Nth order streams is classified as an (N+1) order stream. If a higher-order stream comes together with a lower-order stream, the resultant order becomes the higher order. (Kayitesi et al., 2022)A 1st order stream is a result of overland flow, the upstream flow is usually not concentrated and is usually susceptible to non-point source pollution. Figure 3-6 illustrates an example of the Strahler classification.

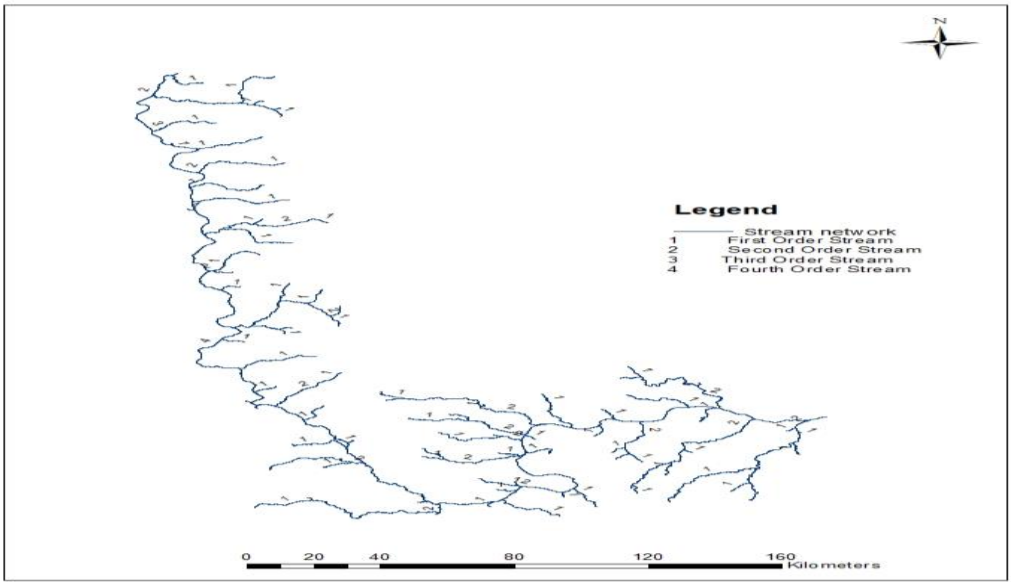

Figure 3: Stream Network of the Black Volta.

Delineating Head Height

A contour map of a 50m interval was generated from the DEM in a GIS environment. Depending on the number of contour lines that traverses a stream reach and the elevation difference (head) is determined (figure 3). The minimum

neighborhood data from the focal statistics was subtracted from the original Digital Elevation model in the raster calculator to get the head height of the surface water using equation (1)

Head height (HT)= Digital Elevation Model (DEM)-Minimum Neighborhood (DEM)…….. (eq. 1)

To obtain a discharge, runoff of the catchment area is required which will be calculated using the Soil Conservation Service (SCS) model developed by the United States Department of Agriculture (USDA) computes direct runoff through an empirical equation that requires the rainfall and a watershed coefficient as inputs. (Obahoundje et al., 2021)The watershed coefficient is called the Curve Number (CN). This model involves the relationship between land cover, hydrologic soil class, and curve number (A, 2021). The annual runoff calculation was approached using the formula (Eq.1);
Q = $(P-Ia)$ 2 $(P-Ia+S)$ (1)

Where Q = actual annual runoff (mm), P = average annual rainfall (mm), S = potential maximum retention, Ia = 0.2S initial abstraction (mm). This is the loss of water before runoff begins by soil and vegetation in the form of infiltration. The constant value of 0.2 was used for Black Volta Basin. The potential maximum retention (S) was calculated by involving CN and the constant value. The equation below is used for the calculation

(Eq. 2). S = 25400 CN − 254 (2)

CN = curve several hydrologic soils and is the function of soil type, Landuse and Land cover (LULC), and antecedent moisture condition (AMC). The final output from all these calculations was the annual runoff in millimeters (mm) which was then integrated with the watershed area to obtain cubic meters (m3) of river discharge. A total of 166 sites were determined in Black Volta Basin, varying in terms of their installed power.

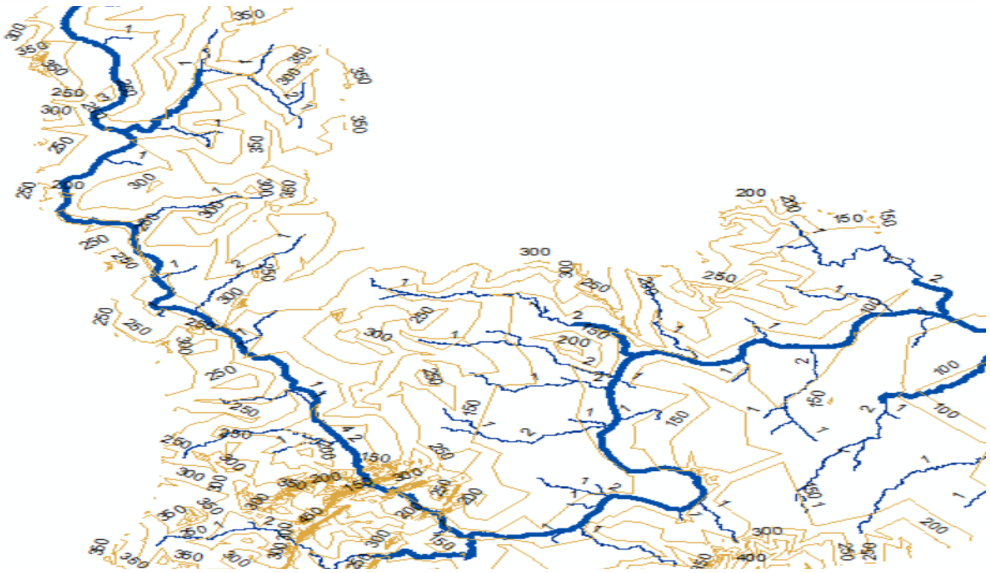

Figure 4: Site selection based on head

Estimation of flow

The SWAT model was selected to estimate the stream flow in the Black Volta Basin for this study. The ArcSWAT software requires several model inputs for it to run. The data requirement for the software include:

1. A DEM maps
2. Land Use/Land Cover map

3. Soil map
4. Climatic Data
5. Rainfall
6. Max Temperature
7. Min Temperature
8. Spatial Reference for the climatic and stream gauge stations
9. Stream flow Data
10. Look Up tables for both soil and land use

The input data were obtained from different sources.

Data Preparation

Daily inputs of maximum and minimum temperature and rainfall are required for SWAT. The data can be read in a .txt format in the SWAT database. There was the need to arrange the data acquired for each station in the required format and then saved it as a .txt file. Missing data were replaced with the value -99.0 so that the model could capture them. Missing data results in the inaccuracy of measured precipitation as well as uncertainty in the data which eventually affects model output. The stream flow data obtained were daily flows. For the software to be able to process map data, all the maps are to be in the same projection (Miracle & Adaobi, 2023). Using the ArcGIS software, data management extension, the DEM, soil, and land use maps were projected into the WGS 1984 UTM Zone 30 coordinate system. The boundary of the Black Volta basin was clipped out of the DEM, Soil, and Land Use maps.

The SWAT Model

SWAT Project Setup

The SWAT model has 6 stages. All the requirements of the first stage must be satisfied before the next stage. The first of the six stages begin with the setting up of the model, "SWAT Project". This stage involves the naming of the project and the selection of a location. The interface of the SWAT project setup is shown in Figures

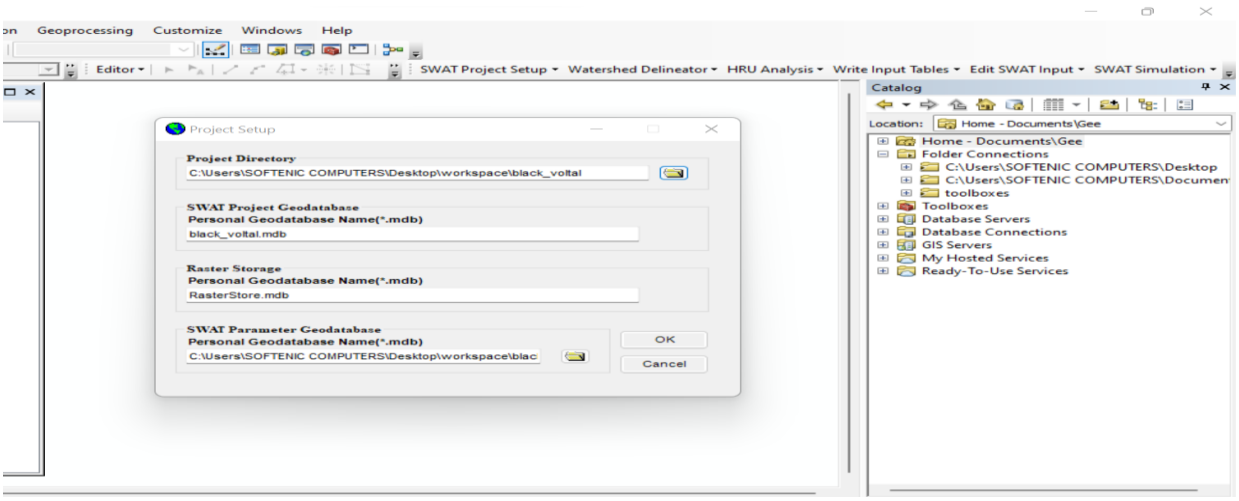

Figure 5: SWAT Project Setup Interface

Watershed Delineation

After the project was set up, the next stage was the watershed delineation. The DEM was input together with the stream network generated. Arc SWAT automatically fills sinks and then generates the stream direction and accumulation and then a stream network based on the DEM. Flow outlets are also added automatically. The proposed small hydropower sites were also added as outlets as well as stream gauging stations. The sub-basins based on the outlet are now created. A sub-basin report is made available. The Watershed Delineator interface is shown in Figure 5. The longest path for each sub-basin is also determined by the model.

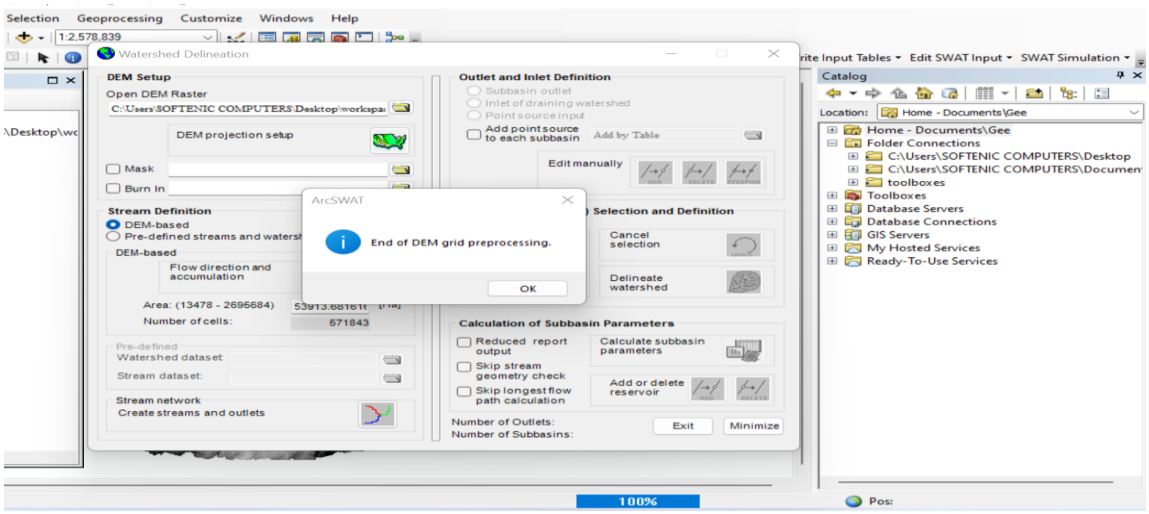

Figure 6: SWAT Water Delineator Interface

HRU Analysis

The Land Cover of the area is added to the model as well as the hydrologic soil classification of the study area. After the shape file of the LULC map was added, the look-up table for the land Use classification was added. The Land Use was then reclassified to correspond to that in the Look Up table. The soil is also reclassified according to the user soil that was added to the soil shape file in the model. A single slope was chosen for the study area and then reclassified. The LULC, soil, and slope interface is shown in Figures. After the LULC, soil, and slope has been determined for the area, the shape files were overlaid and HRU feature classes were created for the basin. The HRU was defined according to the dominant LULC, soil, and slope. After the land use, soil, slope, and HRU were defined, HRUs were then created. The HRU Definition Interface is shown in Figures 3-12 and 3-13. A report on the HRU Analysis is prepared by the model.

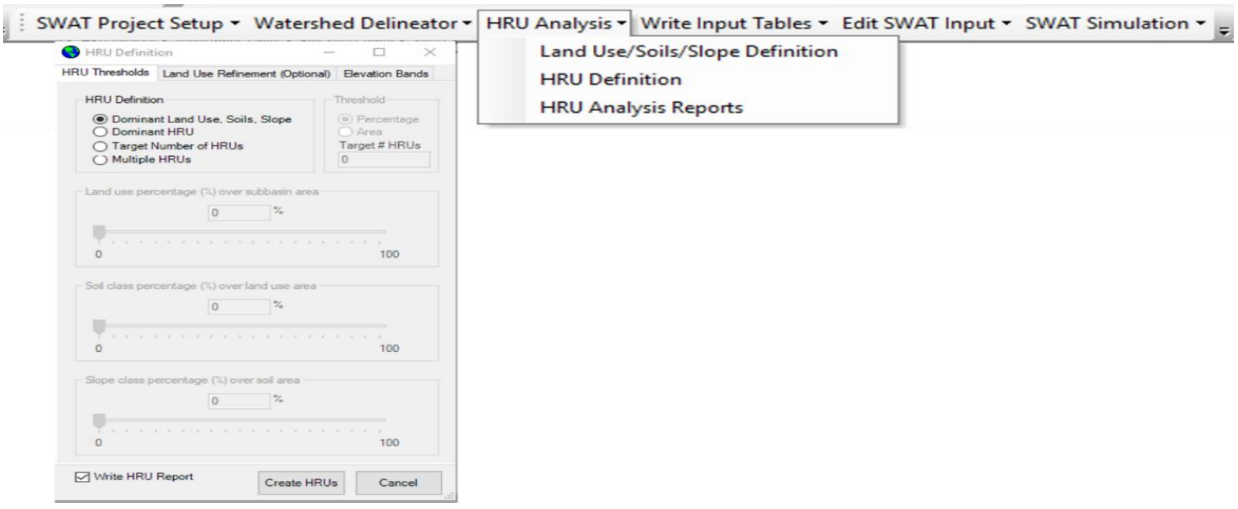

Figure 7: HRU Definition Interface

Input Tables

The rainfall, maximum, and minimum temperature data prepared for the model was inputted at this stage. The station name, location, and elevation of the station are also input. After the selection of the WGEN_user file in the Weather

Generator Data interface, the rainfall and temperature data were input. The data was on a daily time step. Figure **7, shows** the interface for the weather data definition. Relative humidity, solar radiation, and wind speed will be simulated by the model using built-in algorithms because the data was unavailable. The SWAT database table was built after the weather data was defined. Figures show the SWAT Database Tables interface. The database was updated after the tables were generated.

The Edit SWAT input tab helps you to make changes to any of the data that has been entered into the model. The Hargreaves Equation was selected for the computation of Potential Evapotranspiration (PET) for the model.

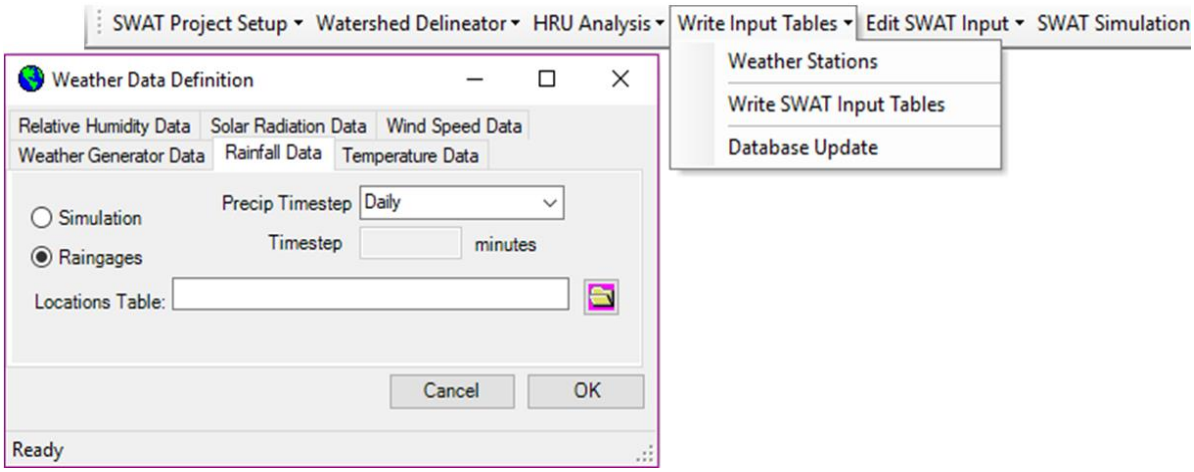

Figure 8: Weather Data Definition Interface

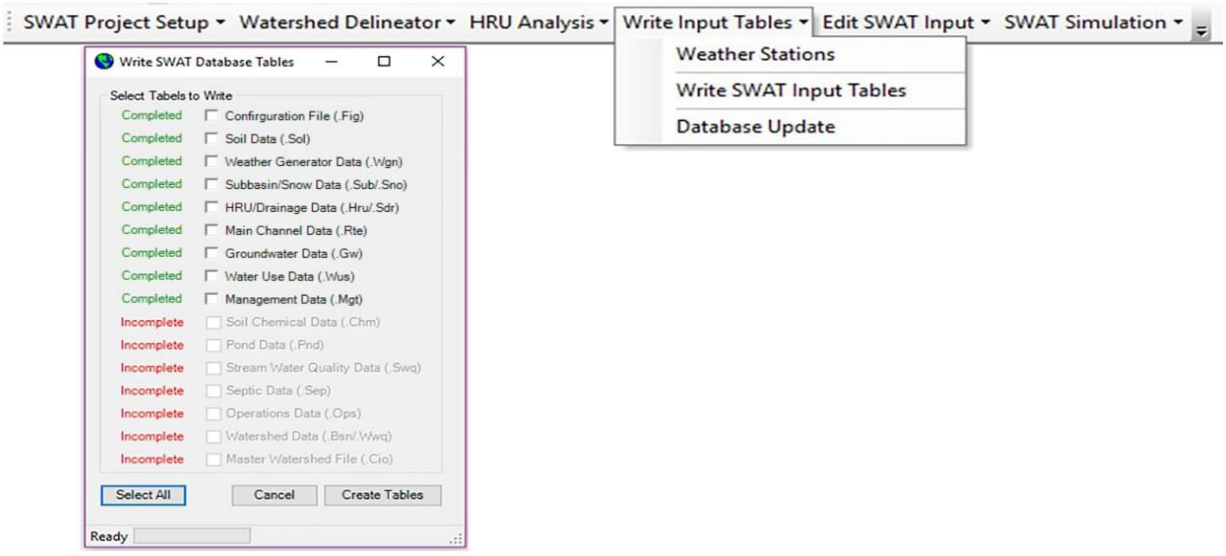

Figure 9: SWAT Database Tables Interface

SWAT Simulation

The starting date for the model was 1st January 2000, with a warm-up period of 2 years and an end date of 12th December 2020. A monthly time step was chosen for the output of the model. The model was then set up. The Figure shows the Setup and Run SWAT Model Simulation interface. Output for reach, sub-basin, and HRU was checked and the SWAT Check was run and the simulation was saved. The SWAT output was read and compared with existing literature to establish the model's ability to predict stream flows for the basin. The model calibration then followed.

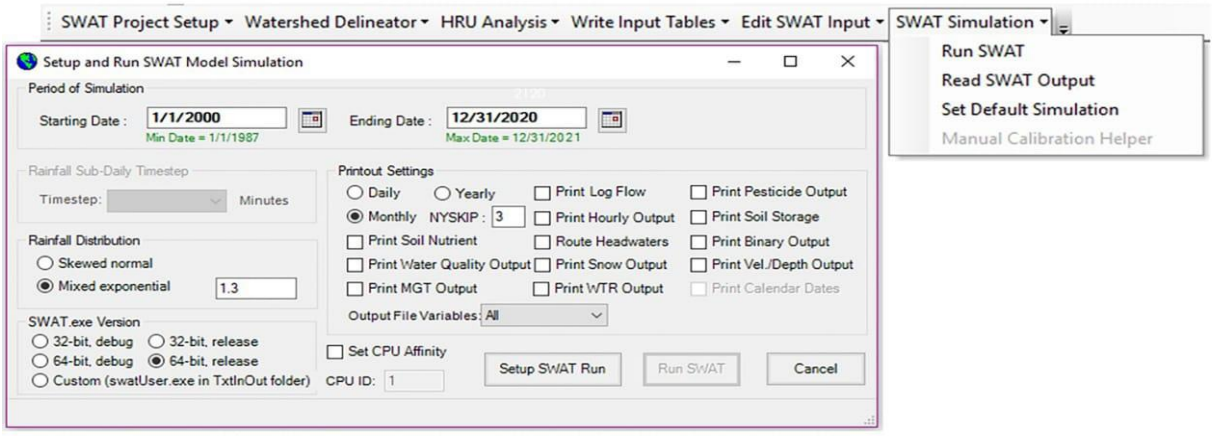

Figure 10: Setup and Run SWAT Model Simulation Interface

Model Calibration and Validation

The SWAT model was calibrated using the manual calibration tab in the ArcSWAT interface according to the procedure proposed by (Neitsch et al., 2005). Stream flow data obtained from the Hydrological Services Department was used for calibration and validation. The prestea gauge station was chosen for calibration and validation. The period of data used for the calibration was 1st January 2000 to 31st December 2020. The interface for the ArcSWAT manual calibration interface is shown in Figure 3-11. The calibration and validation were performed on a monthly time step. The ranges for the model parameters were attained from the Tables In the database for ArcSWAT. Each parameter had thresholds that served as a guide to manual calibration. The values of the parameters varied within their respective maxima and minima thresholds. The values were either replaced (v), multiplied by a factor (r), or by an added increment (a). The parameters that affect surface runoff were first adjusted and then followed by those that characterize the subsurface flow and the base flow.

CN2 was decreased to reduce the surface runoff at the outlets. The reduction was done with the range of values for curve number depending on the LULC being the governing principle for the reduction (Appendix A and B of (Coulon et al., 2021) The efficiency of the model output was determined using the NSE, R2, RSR and the PBIAS criteria. Since the efficiencies were not attained, other parameters of the model were adjusted until the required efficiencies were attained.

The next parameter that was adjusted after the Initial SCS runoff curve number for moisture condition II (CN2) was the Available water capacity of the soil layer (SOL_AWC). This value was decreased and the results were examined, till there was no visible change in the model output with a further decrease in SOL_AWC. The other parameter that was also adjusted for surface runoff was the Soil evaporation compensation factor (ESCO). For the adjustment of the subsurface parameters, the parameters that were adjusted were Threshold depth of water in the shallow aquifer required for return flow to occur (GWQMN), Groundwater "revamp" coefficient (GW_REVAP), Threshold depth of water in the shallow aquifer for "revamp" or percolation to the deep aquifer to occur (REVAPMN), Groundwater delay time (GW_DELAY) and the base flow factor: ALPHA_BF. The adjustment was halted when the efficiency of the model output was desirable.

The model output was checked for validation without any change to the already adjusted parameters. The validation was performed from 1st January 2000 to 31st December 2020. The results attained for the model efficiency were good.

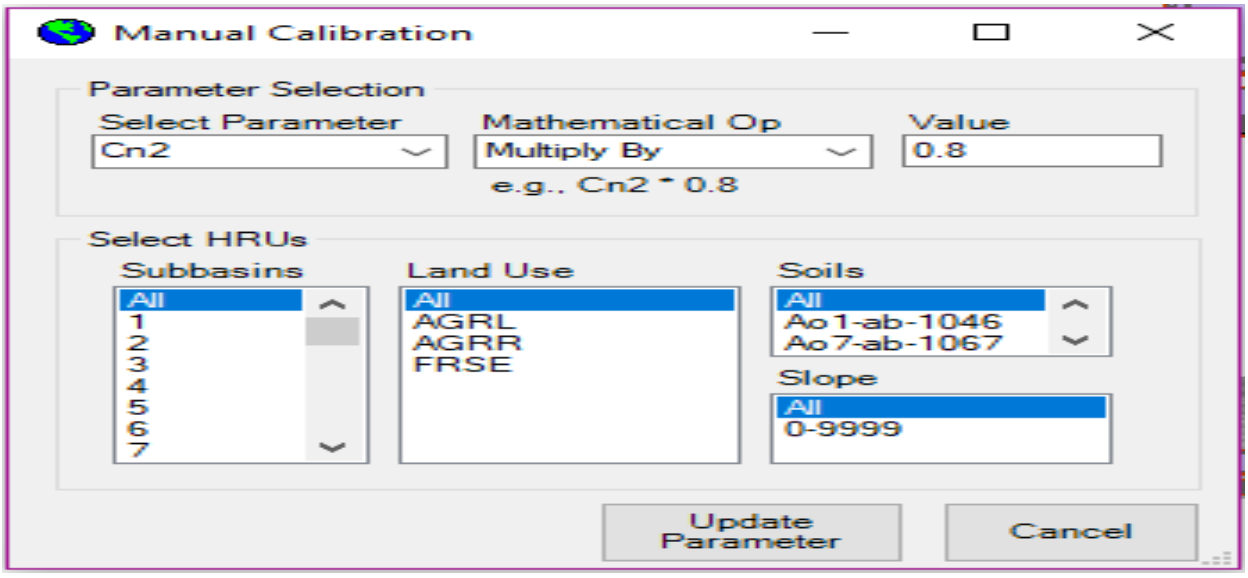

Figure 11: ArcSWAT manual calibration interface

Energy Estimation

Estimation of Firm Power and Firm Energy

The Flow Duration Curve (FDC) was developed for a monthly time series due to the unavailability of daily stream flow data. The data used for the generation of the FDC is that generated from the rainfall-runoff modelling and is presented in the. The data covers a period of 16 years (1997 to 2012). For this study, the dry years of flow were of priority. Hence, the yearly averages of the stream flow data were obtained. The last five (5) average annual flows were selected for the FDC. The FDC was constructed for each site. The procedure used for the generation of the FDC is discussed below:

The stream flow data representing the minimum average annual flows for five (5) years were obtained. The number of the data sets (n) was determined by using the Excel command "Count". The data were then grouped into class sizes with a class interval of 0.49. The classes ranged from 0-0.49 to 85-89.9. The frequency for each class was then determined using the "COUNTIFS" command in Excel. The cumulative number of flows, N in descending order was determined. The percentage dependability was then computed using the equation below.

$$\%\ dependability = \frac{Cumulative\ Number\ of\ Flows\ (N)}{Number\ of\ Data\ Set\ (n)} * 100 \qquad (1)$$

A $\%dependability$ of 90% was used for this study. The flow corresponding to that dependability for each site was determined. An overall efficiency of 75% was used in estimating the power. To estimate the Power at the sites, the equation below was used.

$$Power\ (kW) = \frac{\rho * g * H * Q_{90} * \eta}{1000} \qquad (2)$$

Where,

$$\rho\ is\ the\ density\ of\ the\ water, \frac{1000kg}{m^3}$$

$$g\ is\ the\ acceleration\ due\ to\ gravity, \frac{9.81m^2}{s}$$

$$H\ is\ the\ head\ at\ the\ proposed\ location, m$$

$$Q_{90}\ is\ the\ discharge\ at\ the\ proposed\ location, \frac{m^3}{s}\ corresponding\ to\ 90\%\ dependability$$

$$\eta\ is\ the\ overall\ efficiency\ for\ the\ project$$

For each proposed location, the firm power was derived in KW. The Power and Flow Duration Curves were then plotted against the % availability of flow. A plant capacity factor, C_f of 65% was used in estimating energy. The firm energy at the proposed locations was computed using the equation below:

$$Energy\ (kWhr) = P * T_o * C_f \qquad (3)$$

Were,

$02P\ is\ the\ power\ (kW),$

$T_o\ is\ the\ time\ in\ hours\ for\ the\ number\ of\ days\ the\ project\ will\ be\ run, corresponding\ to\ 90\%\ dependability\ given\ as$

$$T_o(hr) = 0.9 * 365 * 24$$

$$= 7884\ hr$$

$C_f\ is\ the\ plant\ factor$

3. RESULTS

Potential SHP sites along the Black Volta River

In sitting of potential SHP site along the black Volta, two approaches were adopted. The first approach consisted of adopting raster calculator and hydrological modelling using the ArcGIS computer software while the second approach adopted the SWAT Model

Siting of Hydropower Sites (ArcGIS)

In siting a Hydroelectric power, the annual rainfall, the head hight, the land use, the water basin and the flow accumulation were determined. The findings of the study are presented on both tables and figures.

Table 2 Run-off Water of Black Volta Basins

Watershed Object Id/grid code		Pixel Count	Area m²	Mean	Volume (Cubic meter square
1	0	166534	157009230.478902	77583.363777	12920267903.320313
2	1	259211	244385648.826466	116875.044623	30295297191.876953
3	3	944346	890334939.206585	54092.568237	51082100444.061523
4	5	5	4714.029282	20741.728516	103708.642578
5	6	6258	5900079.048945	27879.061123	174467164.505859
6	8	119823	112969826.123635	41854.700395	5015155765.394531
7	10	476937	449658996.702873	68175.023312	32515191093.133789
8	12	160249	151083695.671836	78724.661843	12615548335.746094
9	14	119672	112827462.439329	69074.457063	8266278425.584961
10	16	298211	281155077.223534	97077.352097	28949534246.070313
11	18	492116	463969846.796183	134149.894325	66017309395.738281h
12	19	1	942.805856	114079.507813	114079.507813
13	22	915877	863494199.282583	198787.002248	182064443257.4375
14	24	643919	607090604.205413	197142.629668	126943884953.03125
15	26	901420	849864055.017547	210847.299837	190061973018.78125
16	29	358353	337857307.035237	222512.356369	79737970442.015625
17	41	200015	188575313.354856	83026.716953	16606588791.410156
18	43	455623	429564032.680947	68018.338143	30990719279.568359
19	45	243730	229790071.364543	162376.213712	39575954568.039063
20	47	1	942.805856	40540.652344	40540.652344
Total			6,375,536,985		913832942604.518555

As observed from Table 2, the analysis of runoff water within the watershed reveals notable disparities in area, mean runoff, and volume of runoff water across different objects. The mean runoff values provide valuable insights into the patterns of runoff within the watershed, ranging from approximately 41,000 to 134,000 cubic meters per square meter. These variations highlight significant differences in the runoff potential among different areas, which can be attributed to factors such as topography, vegetation cover, and land use practices.

Furthermore, the study estimates a total runoff volume of approximately 913 billion cubic meters, covering an area of approximately 6,375.536985 square kilometers (equivalent to 6,375,536,985 square meters). These figures indicate the extensive coverage of runoff water within the watershed, revealing areas with a potential hydro power potential energy capacity.

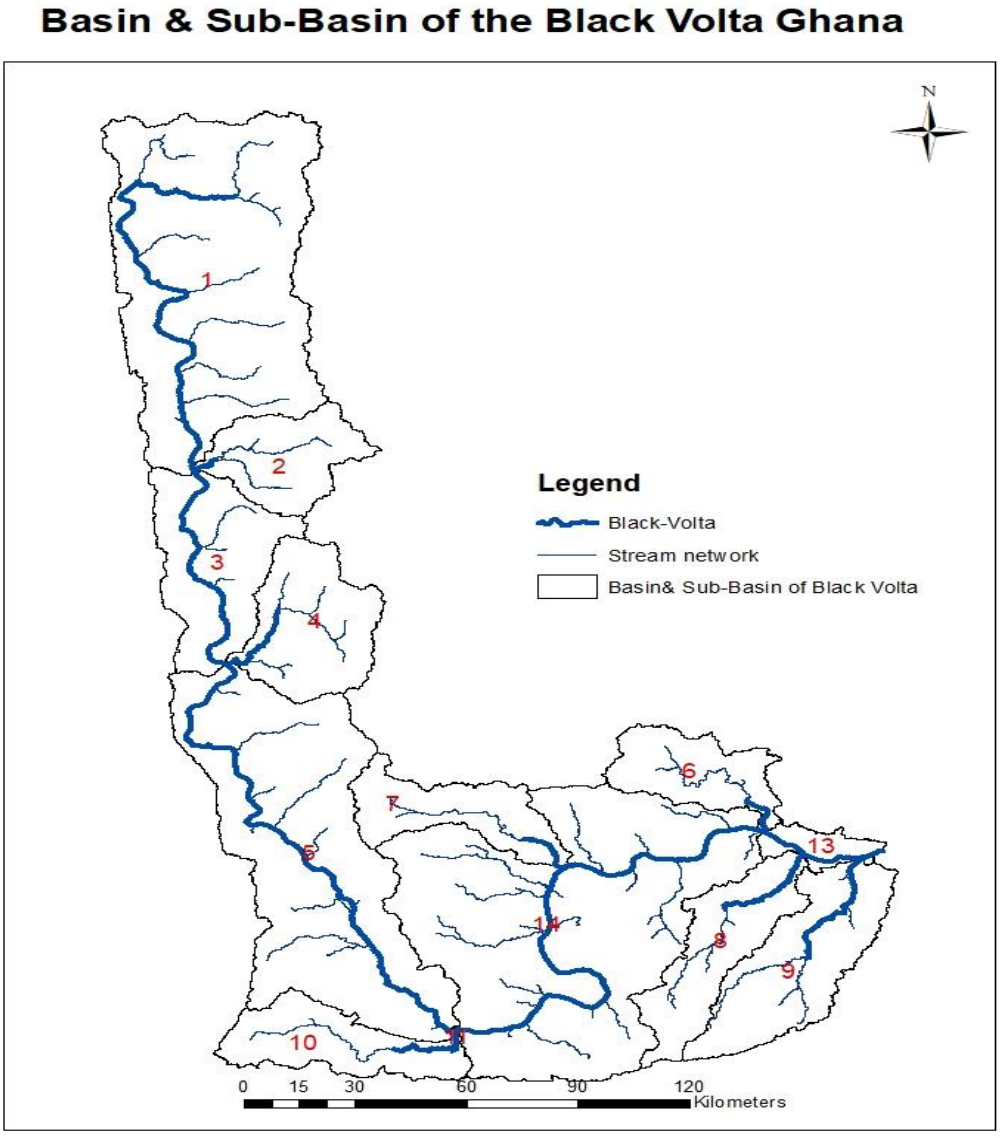

Figure 12: Sub-basin of Black Volta Basin-Ghana

Table 3: Statistics of Streams in the Black Volta Basin-Ghana

Stream Order	**Frequency**	**Percentage (%)**
1st order	85	50.30
2n order	37	1.89
3rd order	12	7.10
4th order	35	20.71
Total	**169**	**100**
Stream Magnitude	**Frequency**	**Percentage (%)**
1- 20	125	73.96
21-46	28	16.57
47-56	8	4.73
57-85	5	2.96
Total	**169**	**100**

The findings from the table 3 reveal important insights about the stream orders and stream magnitudes within the studied watershed. The distribution of stream orders indicates that smaller tributary streams of the 1st order are the most prevalent, comprising 50.30% of the total. This suggests a dense network of smaller streams in the watershed. Additionally, the presence of 2nd, 3rd, and 4th order streams indicates the occurrence of larger and more significant watercourses.

Regarding stream magnitudes, the majority of streams fall within the 1-20 range, accounting for 73.96% of the total. These streams likely possess higher flow rates due to their larger contributing drainage areas. Streams in the higher magnitude ranges (21-46, 47-56, and 57-85) represent smaller percentages, suggesting lower flow rates but still holding potential for hydropower development. These findings have important implications for the siting of mini hydroelectric power projects. Higher stream orders and larger stream magnitudes typically indicate greater potential for energy generation. Therefore, areas with 2nd, 3rd, and 4th order streams (figure 4.2), as well as streams with higher magnitudes, could be suitable for the development of mini hydroelectric power plants. The graphical representation of the stream network is shown in figure

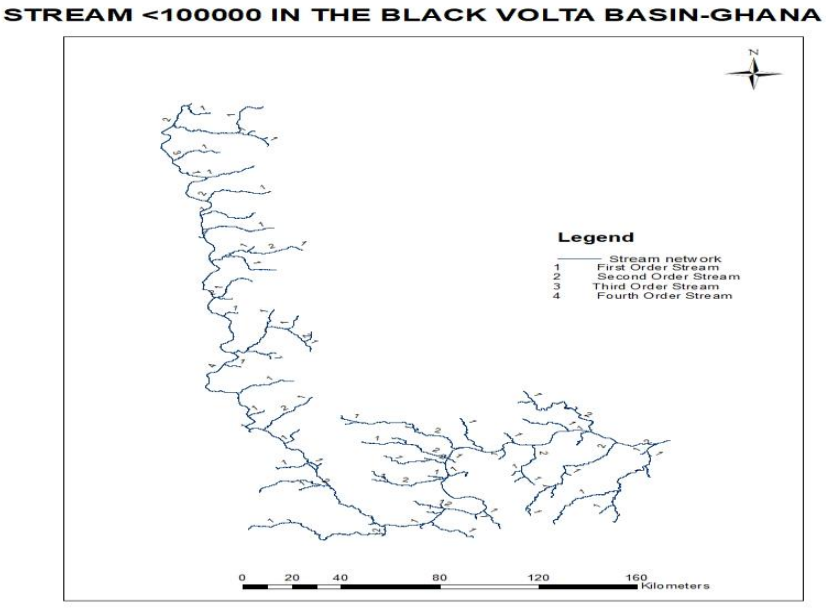

Figure 13: Steam Network

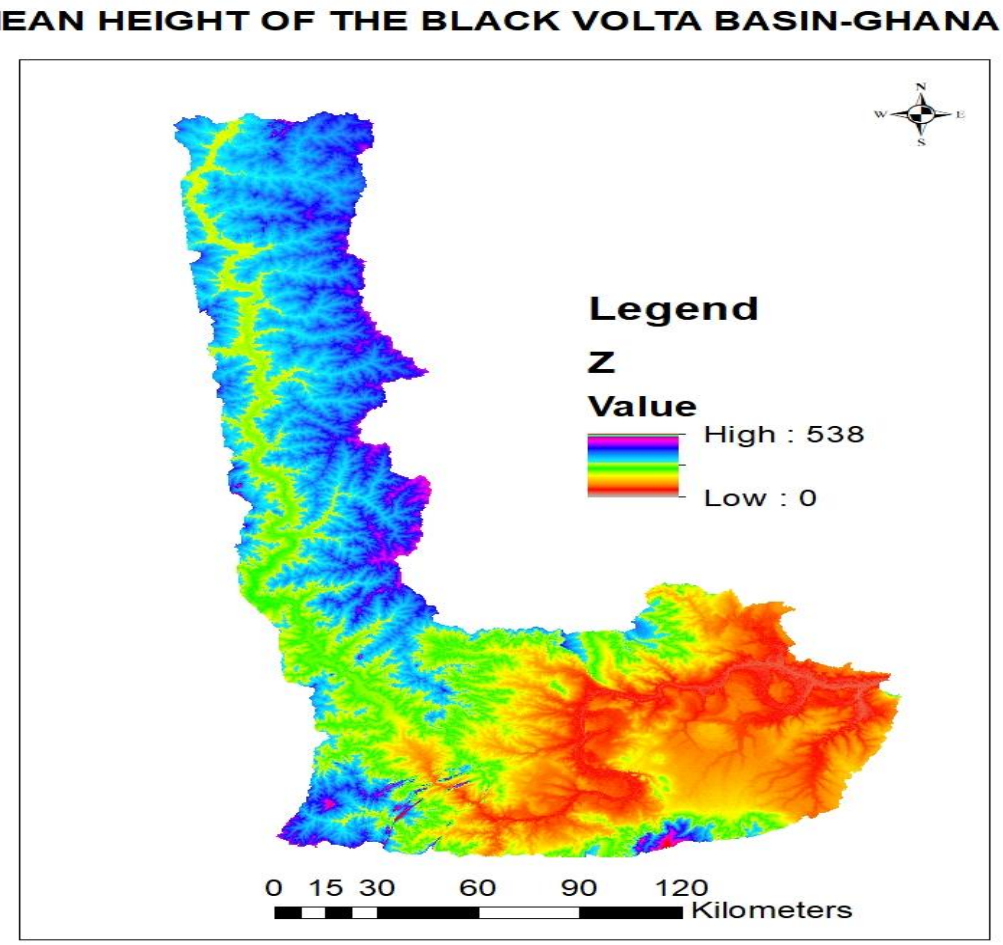

Figure 14: Height off the Black Volta

Head Drop

The falling height/head drop of the area indicate a low land area with the highest point of 538 feet above sea level

Table 4: Mini hydropower potentials Sites in Black Volta Basin, Ghana

Hydropower Plant Classes	Installed Power Potential (MW)	Number of Site
Small	<50	31
Medium	51-100	68
Large	>101	62
Largest	192	5
Total		**166**

As a result of the analyses made presented in Table 4 from the study, a total of 166 sites were determined in Black volta Basin, varying in terms of their installed power. The classifications of hydropower potential sites are Small (> 50 MW) Medium (51-100 MW), Large (<101 MW) and Largest (192 MW). The analysis revealed that potential site in the Black Volta Basin with small capacity of 50 MW were 31 whiles potential site for mini-hydro capacity of 51-101 MW were also 68. Moreover, potential site with install capacity greater than 101 MW were 62 and potential sites with the highest install capacity of 192 MW were five (5)

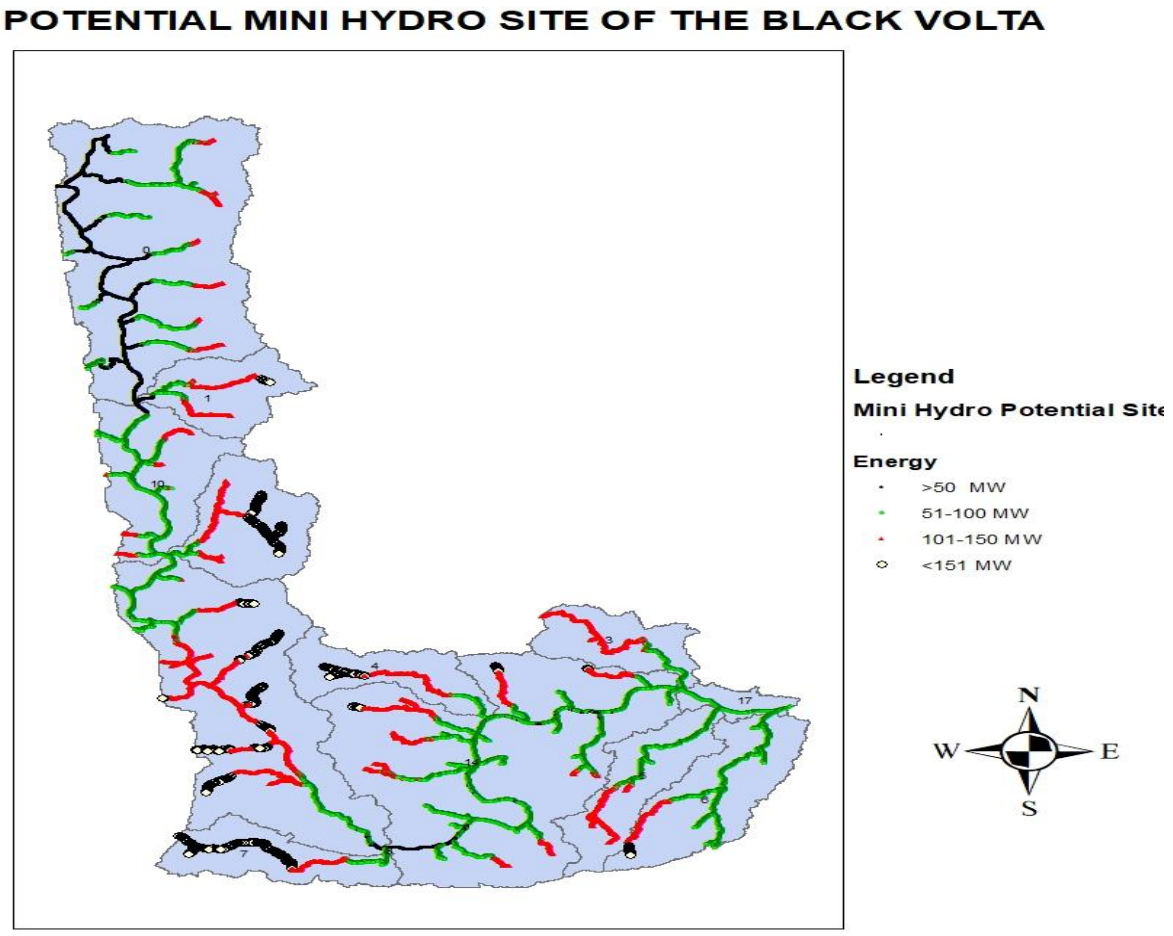

Figure 15: Mini-hydro potential Sites

SWAT

The results presented in this section are obtained from the output map of the SWAT model and the SWAT-CUP model. It also contains results obtained from the calibration and validation of the model.

Stream flow Data in the Basin

The mean runoff in the Black Volta is estimated at 7km^3/7million m^3 per annum. The driest and wettest months are March and September, respectively. Monthly flows in Lawra (upstream), Bui (Midstream) and Bamboi (downstream) were used to assess the runoff from the basin within Ghana.

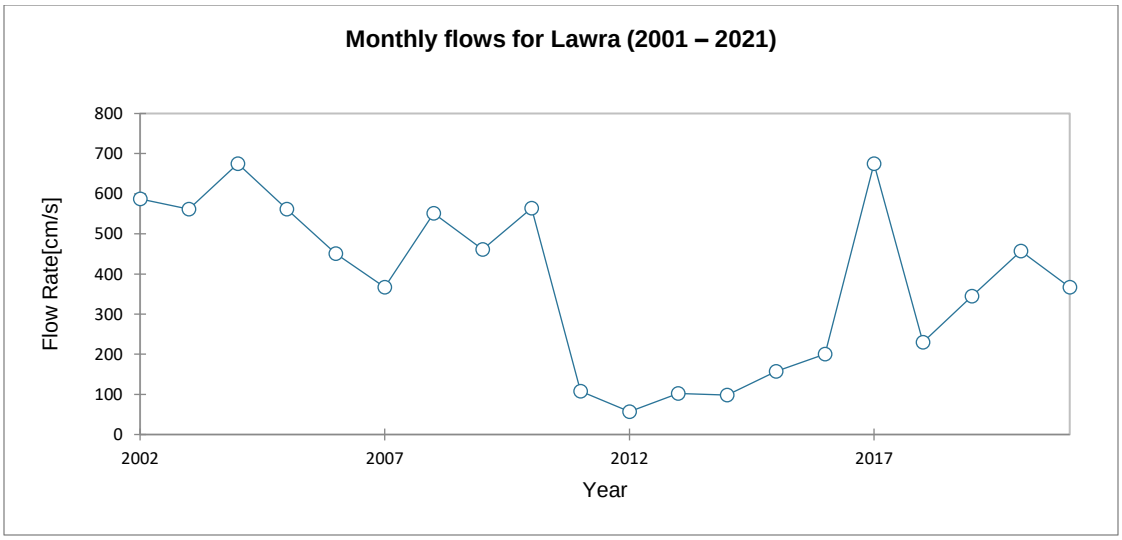
Monthly flows for Lawra (2001 – 2021)
Flow Rate[cm/s]
800
700
600
500
400
300
200
100
0
2002
2007
2012
2017
Year

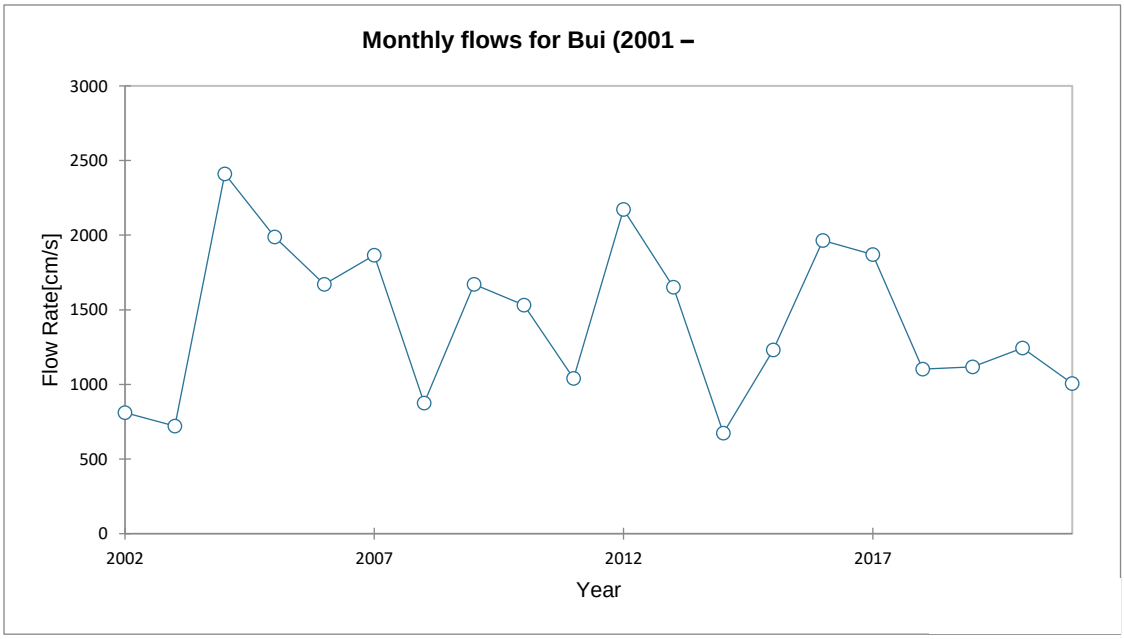
Monthly flows for Bui (2001 –
Flow Rate[cm/s]
3000
2500
2000
1500
1000
500
0
2002
2007
2012
2017
Year

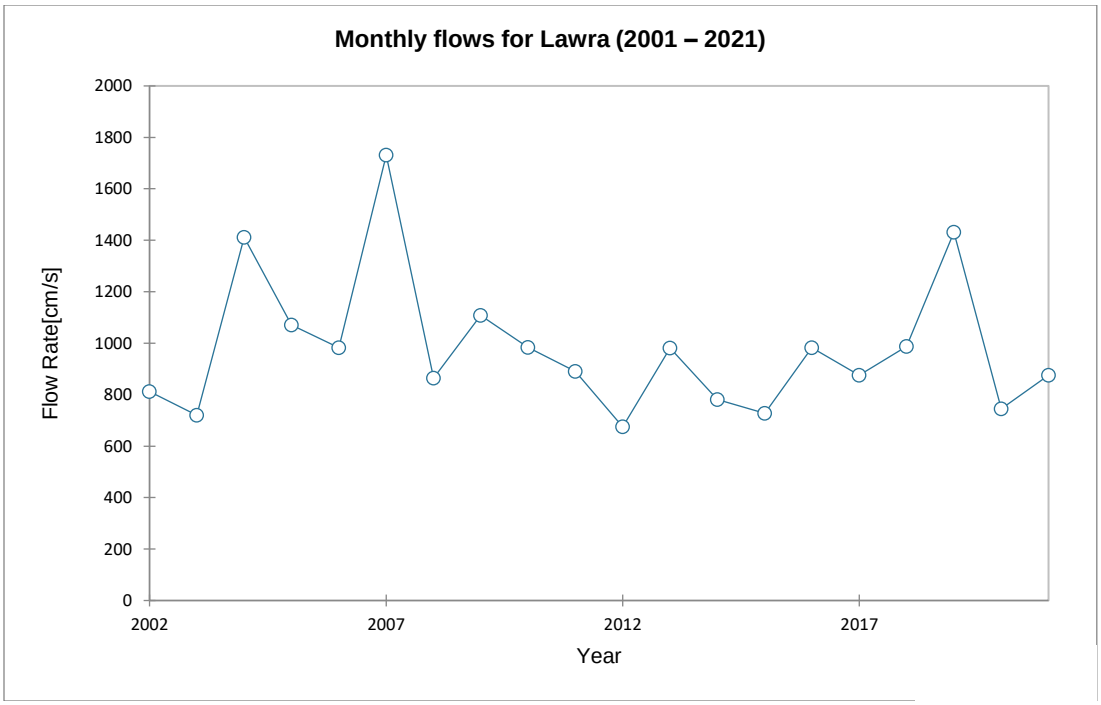

Sub basin and HRU Delineation

The sub basins were delineated (57), the outlets were selected based on the 23 proposed locations of the hydropower sites, stream gauge stations and default nodes presented by the SWAT model. The sub basins are as shown in Figure 16 The dominant land use and soil in the basin was used to create an HRU. 57 HRUs were created for this study with a uniform slope between 0-99.99%. The 57 sub basins each consisted of different land use classes as well as soil group whiles the HRUs were characterized by the dominant land use and soil in that particular unit.

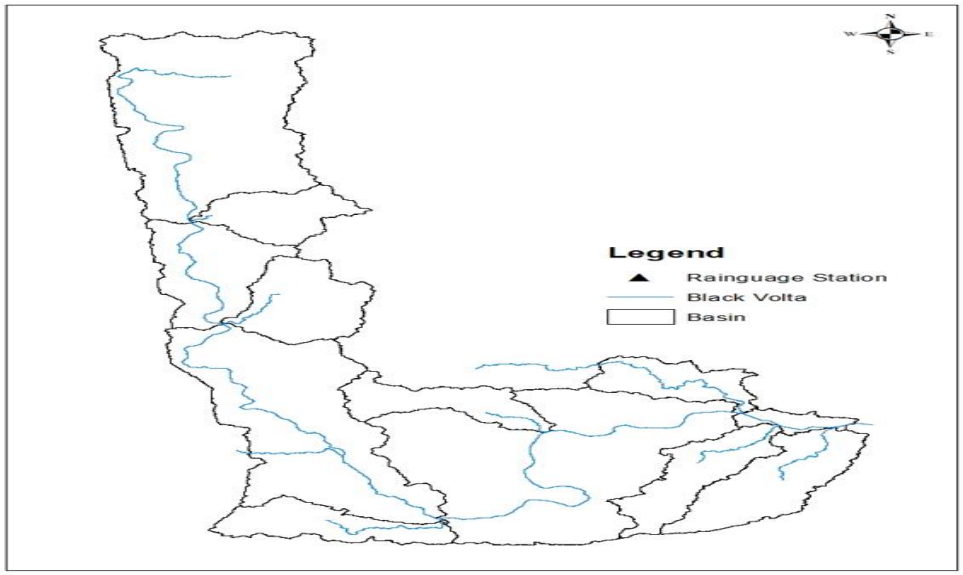

SOIL DISTRIBUTION IN THE BLACK VOLTA BASIN

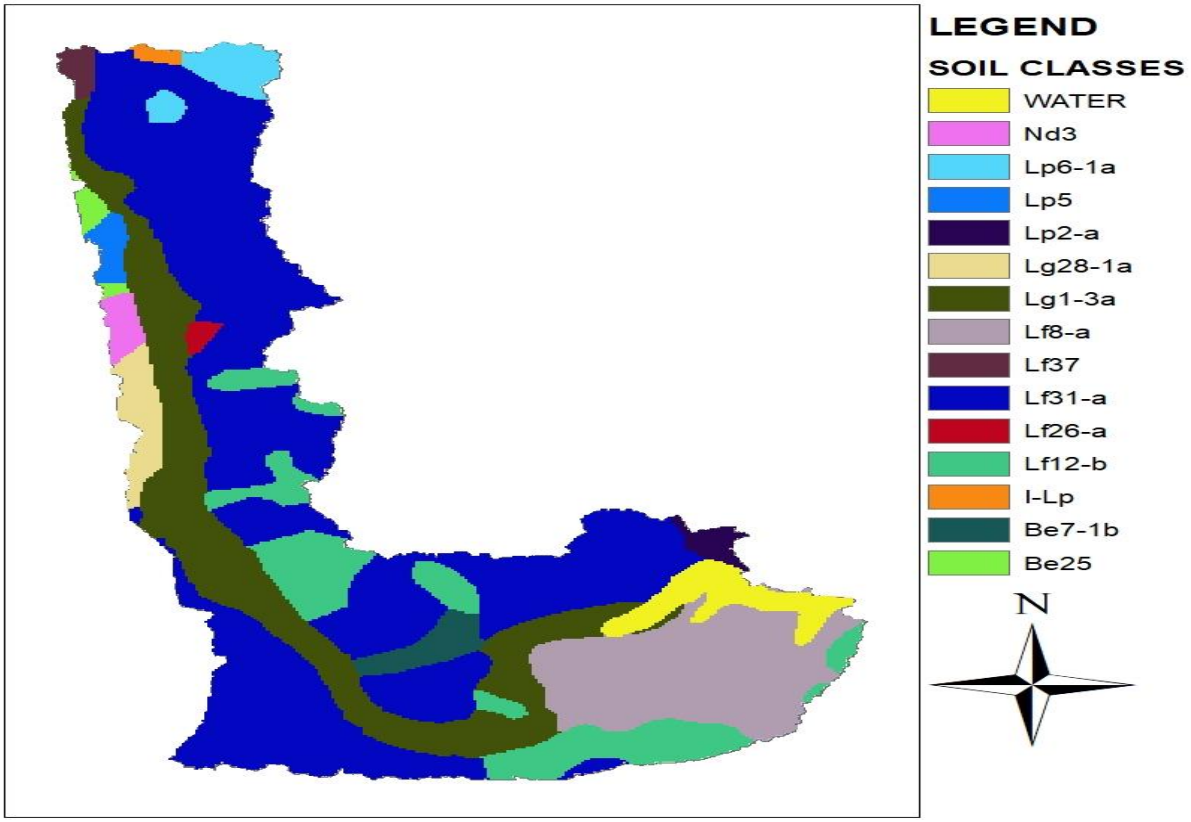

SWAT Model Sensitivity, Calibration and Validation

The SWAT model was calibrated and validated on a monthly time step using stream flow data obtained from the Hydrological Services Department although the data inputs was on a daily time step. The period for calibration was 20 years 1st January,2001 to 31st December,221. 1st January, 2009 to 31st December, 2012 was used for the validation. The Bui station was chosen for the calibration and validation of the model as it had reliable data compared to the other stations in the basin. Manual calibration was used to assess the efficiency of the model.

According to Arnold *et al.* (2012), manual calibration is difficult but gives better insight as to the sensitive parameters in the basin. The procedure followed for the manual calibration was that proposed by (Neitsch *et al.*, 2002).

Model calibration parameters were selected based on literature review in diverse basins around the world and specifically those with similar characteristics as the Black Volta Basin on the application of SWAT in the area (Habte et al., 2013;Adjei et al., 2014; Silva et al., 2015; Swami & Kulkarni, 2016; Awotwi et al., 2017; Almeida et al., 2018; Bennour et al., 2022,). The parameters used for calibration and validation of the model which were sensitive to the outcome of the output of the model with their respective descriptions are given in Table 4-3. The respective ranges and the values that were fitted are shown in Table 4-4. In varying the parameter values during calibration, it was ensured that their respective maxima and minima thresholds were maintained. The values were either replaced (v), multiplied by a factor (r) or by an added increment (a).

Table 5: Model sensitive parameters, their descriptions and units.

Parameter	Description	Units
CN2	Initial SCS runoff curve number for moisture condition II	
ALPHA_BF	Base flow alpha factor	Days
GW_DELAY	Groundwater delay time	Days
GWQMN	Threshold depth of water in the shallow aquifer required for return flow to occur	mm H_2O
REVAPMN	Threshold depth of water in the shallow aquifer for "revap" or percolation to the deep aquifer to occur	mm H_2O
GW_REVAP	Groundwater "revap" coefficient	
ESCO	Soil evaporation compensation factor	
SOL_AWC	Available water capacity of the soil layer	mm H_2O/mm soil

Table 6: Parameters sensitive to the model, their fitted values and the minimum and maximum ranges

Parameter	Fitted Value	Minimum	**Maximum**
r__CN2_AGRR	41.36	35	98
r__CN2_AGRL	40.38	35	98
r__CN2_FRSE	37.47	35	98
v__ALPHA_BF	0.39	0	1
v__GW_DELAY	27.9	30	450
v__GWQMN	3000	0	5000
r__REVAPMN	80	0	500
r__GW_REVAP	0.1	0.02	0.2
r__ESCO	0.14	0	1
r__SOL_AWC_SANDY_LOAM	0.54	0	1
r__SOL_AWC_SANDY_CLAY_LOAM	0.76	0	1

The selection of these parameters was based on several factors. Firstly, they have a direct impact on the amount of water present in the system. Secondly, in the evaluation of water balance components (WBC), these parameters play a crucial role. Lastly, the USGS consistently examines these parameters as part of their efforts in model validation and calibration.

The curve number (CN) is a measure of the surface runoff generated by water. It is influenced by various factors, including land use, hydrologic soil group, soil type, soil permeability, and antecedent soil moisture condition (Neitsch et al., 2005). A CN value of 1 indicates a highly permeable surface, while a value of 100 represents an impermeable surface (Neitsch et al., 2005). Higher CN values are associated with increased surface runoff and decreased base flow (da Silva et al., 2015). In the case of the Volta basin, which is characterized by extensive vegetation cover as evident from the land use and land cover (LULC) map, the model observed CN2 values of 44.8, 73.32, and 39.54, respectively.

The soil's available water capacity, SOL_AWC, represents the water quantity accessible for plant uptake when the soil is at field capacity. Higher SOL_AWC values indicate a larger amount of water retained in the soil, which leads to a reduction in available water for runoff and deep percolation. In the context of this basin, these elevated values signify the soil's ability to maintain its moisture content.

To account for the soil's evaporation demand across different depths, the soil evaporation compensation factor, ESCO, is adjusted. This factor considers factors such as cracks, crusting, and capillary action that influence soil evaporation (Neitsch et al., 2005). Lower values of ESCO enhance the model's capability to extract more evaporative demands from lower soil levels. This results in increased evapotranspiration (ET), decreased base flow and surface runoff, and a reduction in the amount of soil water (da Silva et al., 2015). For model calibration, an ESCO value of 0.14 was chosen.

The parameters responsible for the response of the basin to subsurface flow are ALPHA_BF, GW_REVAP, GQWMN, GW_DELAY and REVAPMN. ALPHA_BF, the base flow recession constant, is the indication of the response of groundwater to changes in recharge. Depending on the type of response, the values range from 0.1-0.3 for areas with slow responses to 0.9-1.0 for areas with quick responses to recharge (Neitsch et al., 2005). The fitted value for the Black Volta basin was 0.4, indicating a moderate response to groundwater recharge. The value of ALPHA_BF (days) is a representation for how long the base flow recession, declines in one log cycle.

GW_REVAP represents the amount of water that moves from the shallow aquifer to the overlying unsaturated zone. A value approaching 0 is an indication of the restriction of water from the shallow aquifer to the root zone (Neitsch et al., 2005). As the value for GW_REVAP approaches 1, the rate of PET is approached by the rate of transfer from the shallow aquifer to the root zone. The range of values for GW_REVAP should be between 0.02 and 0.2.

GWQMN describes the threshold at which return flow can occur. Only when GWQMN is greater than or equal to the depth of water in the shallow aquifer will groundwater flow into the stream reach. The fitted value for the calibration was 3000mmH2O.

GW_DELAY represents the time in days it takes for the aquifer to recharge. Shallow aquifer recharge occurs when water moves through the lowest depth of the soil profile by percolation or bypass flow and enters the vadose zone (Neitsch et al., 2005). The time depends on the hydraulic properties of the geologic formations in the groundwater and vadose zones and the depth of the water table. A value of 28 days was fitted for the calibration.

REVAPMN is the depth of water that must be available in the shallow aquifer for the movement of water from the shallow aquifer to the unsaturated zone or the deep aquifer (Neitsch et al., 2005). 80mmH2O of water must be available in this model for water to move from the shallow aquifer to the unsaturated aquifer.

SWAT Model Performance

From Figure 4-11, it can be observed that the model predicts the peaks well with a little lag between the simulated and calibrated for between September, 2003 and October,2003. This can also be seen in the scatter plots for both calibration and validation, Figure 4-12 and Figure 4-13 respectively. The validation data has high peaks compared to the calibration and hence the better performance outcome. In general, the model performs satisfactorily and can be used for the management of water resources in the basin.

The main evaluation criteria for the model were the NSE. With an NSE of 0.60 for the calibration and 0.67 for validation, the model can be described as satisfactory (Gholami *et al.*, 2016; Moriasi *et al.*, 2007) based on the main criteria for efficiency that was used. Other performance indicators estimated for the calibration and validation period were R^2, RSR and PBIAS (Arnold *et al.*, 2012; Krause *et al.*, 2005; Moriasi *et al.*, 2007; Sittichok *et al.*, 2018). They also confirm the model as satisfactory. A report of the efficiency criteria is shown in Table 4-5. (da Silva *et al.*, 2015; Swami & Kulkarni, 2016) suggest that an $R^2 \geq 0.7$ is an indication of a very good model. The model overestimates flow as depicted by the PBIAS. The overestimation in flows compared to the observed data could be attributed to the inconsistencies in the observed data as reported early on in this report and by (Water Resources Commission, 2009).

Table 7: Model Performance Criteria

Criteria		Calibration	Validation	Performance Ranges	Performance Rating
NSE		0.6	0.63	0.5<NSE<0.65	Satisfactory
	R^2	0.7	0.8	$R^2 \geq 0.7$	Very Good
RSR		0.63	0.61	0.6<RSR<0.7	Satisfactory
PBIAS (%)		10.10%	14.4%	±10<PBIAS<±15	Good

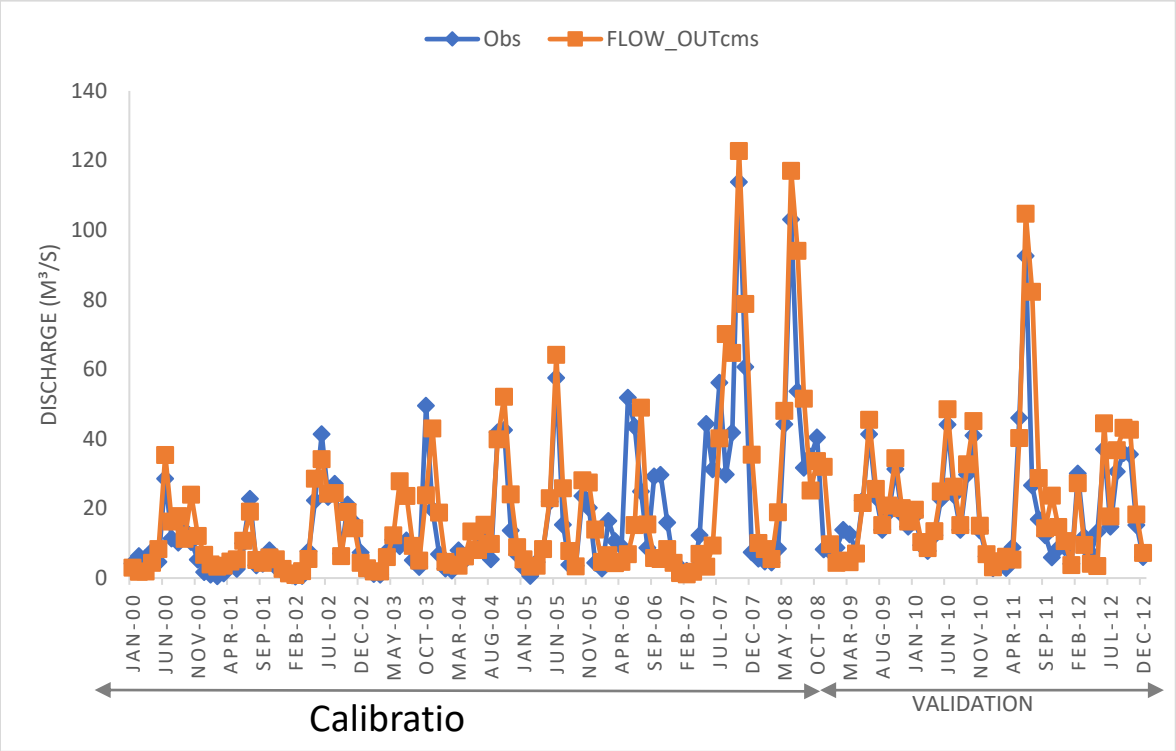

Figure 16: Observed flows and simulated flows for SWAT model

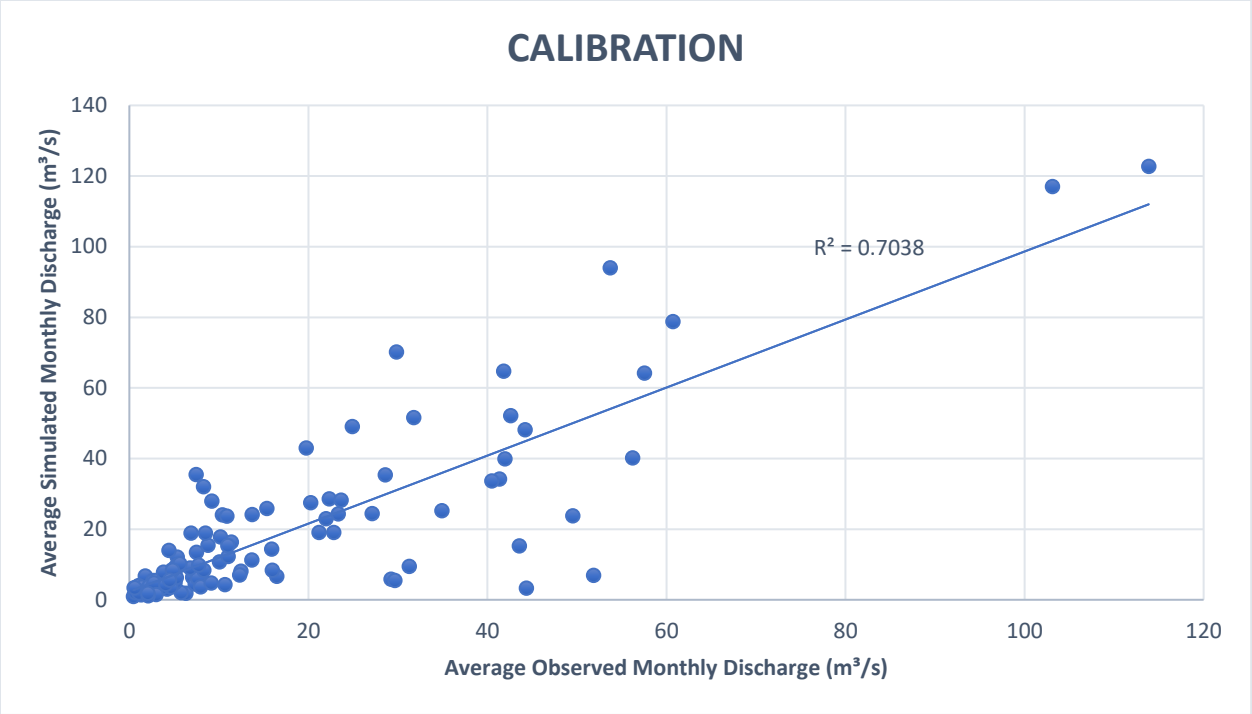

Figure 17: Scatter plot of average observed monthly discharge against average simulated monthly discharge for Prestea station during calibration

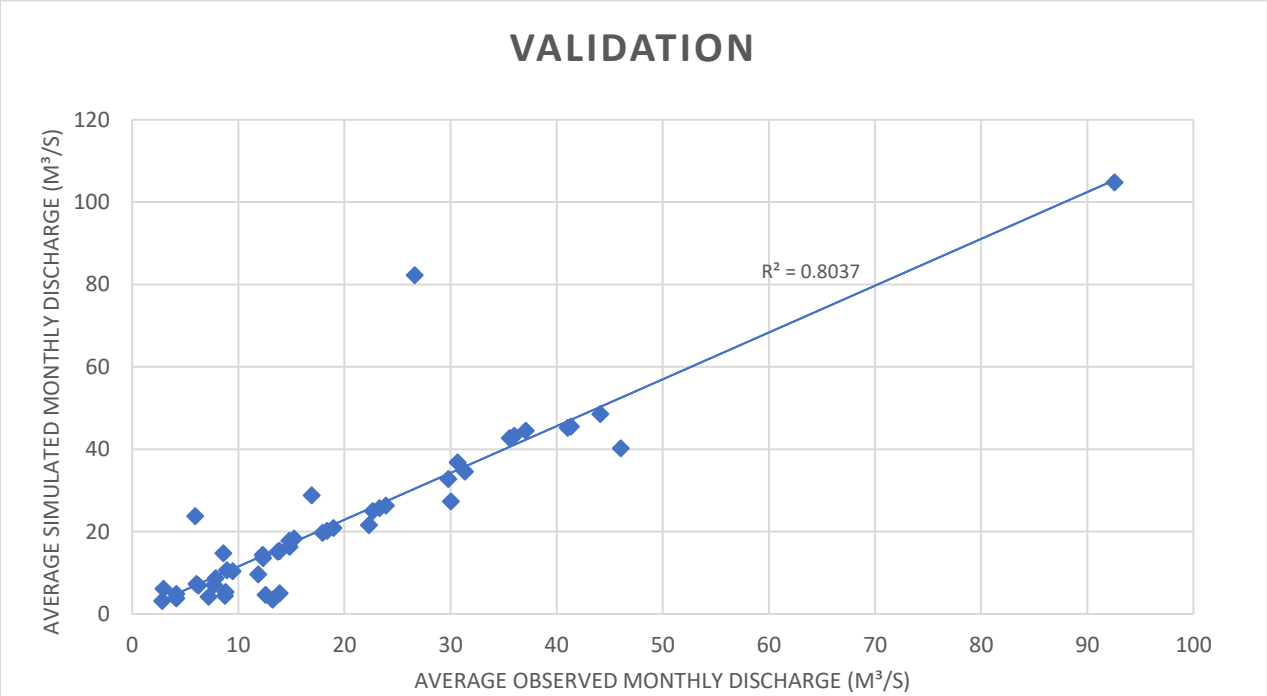

Figure 18: Scatter plot of average observed monthly discharge against average simulated monthly discharge for Prestea station during validation

SWAT Simulation

The model simulation was performed from the 1st January, 1995 to 31st December, 2012. The warm up period for the model was two (2) years, 1st January, 1995 to 31st December, 1996. The SWAT model estimated average annual values for rainfall, Potential Evapotranspiration (PET), actual Evapotranspiration (ET), stream flow etc. An annual rainfall of 1201mm was estimated by the model.

Table 8: Comparison of model output with existing literature

Basin Parameter (mm)	SWAT Model	(Ghana Statistical Service)
Rainfall	1201	1118
ET	1118.2	1088
PET	1505.1	1700
Groundwater Recharge (Shallow & Deep)	488.62	4897.54

A higher record of ET in the model could be attributed to the over estimation on the part of the model due to the unavailability of some climatic data (relative humidity, solar radiation, etc.) or changes in the climate in recent times. Due to the high record of ET in the model, the groundwater recharge estimation was lesser than that reported by (Water Resources Commission, 2009). The high record of ET also resulted in the reduction of surface runoff per the model output.

Energy Estimation

Estimation of Firm Power and Firm Energy

In order to estimate the hydropower at the proposed location, the generation of FDC for each proposed site was crucial (Kusre *et al.,* 2010). In the estimation of hydropower, dry years are taken into consideration (Froend, 2012) to ensure the availability of the firm or base power all year round. For the simplification of the FDC, a monthly interval was used for the construction (Searcy, 1959; Vogel & Fennessey, 1994). For each of the proposed sites, an FDC was constructed. The Black Volta River is a perennial river as shown in the FDC's of the proposed locations, since the 100% availability of flow for each site is above 0m^3/s.

To estimate the hydropower and hence the energy at a given point, the percentage dependability of the flow at the point must be known. The percentages of dependability usually used are 90%, 75% and 50% of flow (Kusre *et al.,* 2010; Pandey *et al.,* 2015). For this work, a dependability of 90% was adopted from (Hidayah *et al.,* 2017). The results therefore represent the minimum energy available even in the driest year.

The overall efficiency of a hydropower project is dependent on a number of factors. These factors include: the efficiency of the turbine, the penstock and the generator (Fagbohun, 2016). An overall efficiency of 75% was adopted for the study. Other losses that occur to reduce the overall efficiency of the hydropower project include hydraulic head losses, transformer efficiency, (Fagbohun, 2016) etc.

For the estimation of energy, a plant capacity of 60% was used based on Kusre *et al.,* (2010) and Reichl and Hack, (2017) work on SHP. To ensure constant supply of power when the flow is available, the proposed locations are expected to run 328 days out of 365 days. The estimated firm power and firm energy are shown in Table 4. The minimum amount of energy to be harnessed at all the 9 sites annually is 25GWhr of energy. The average power and energy that can be harnessed from each of the 9 sites is 550kW and 2.8GWh respectively for a dry year. A typical flow duration curve showing the flow amounting to 90% dependability constructed for the proposed site is as shown in Figure 4.

Of the nine (9) proposed locations for SHP harnessing, the site with the maximum power potential is Site 6. A firm power of 807kW and an annual firm energy of 4.14GWh is expected to be harnessed from this location. The site is

located about 600m downstream of Hemang. Site 4 recorded the minimum amount of power, 329kW and an annual energy of 1.69GWh. The power and energy reported was estimated based on the 90% dependability of the flows for dry years and hence it represents the minimum amount of energy that can be harnessed from these sites.

Table 9: Flow and Power Duration Cuvrve for Site 1

Site	Flow (m^3/s)	Head (m)	Firm Power (kW)	Firm (MWh)	Energy	Firm Energy (GWh)
1	44.87	34.56				
2	52.76	41.2				
4	67.5	48.51				
5	98.12	67.21				
6	67.44	46.71				
7	30.45	54				
6	75.01	37				
7	88.12	67				
8	78.98	54				
9	98.34	55				
10	102	34				

Figure 19: FDC and PDC showing 90% dependability

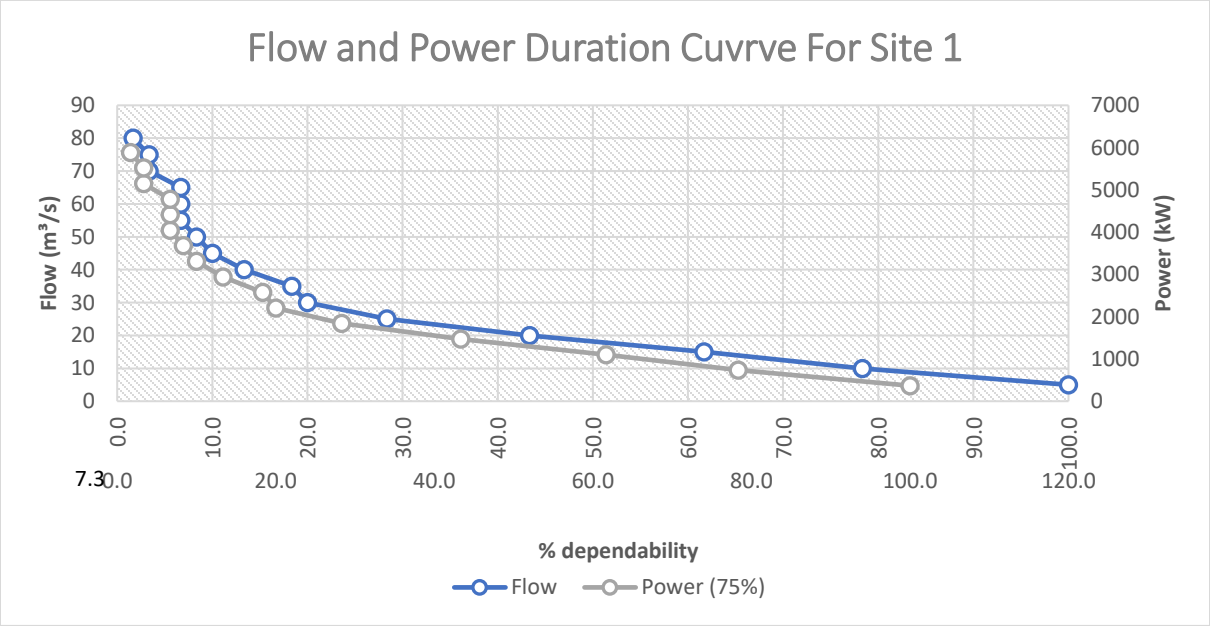

Table 10: Firm power and firm energy for proposed locations

Site	Flow (m3/s)	Head (m)	Firm Power (kW)	Firm Energy (MWh)	Firm Energy (GWh)
1	11.81	13.4	1657.395	14.475	0.014
2	5.10	5.01	253.880	2.220	0.002
4	8.54	7.76	598.594	5.231	0.005
5	6.71	2.48	106.049	0.927	0.001
6	13.1	9.12	1279.773	11.187	0.011
7	17.55	13.78	3484.546	30.447	0.030
6	21.67	15.32	4989.927	43.568	0.044
7	9.32	6.34	330.489	2.886	0.003
8	8.90	4.31	303.567	2.654	0.003
9	12.71	8.44	1427.834	12.476	0.012
10	23.01	17.41	9999.802	87.598	0.088
Site	Flow (m3/s)	Head (m)	Firm Power (kW)	Firm Energy (MWh)	Firm Energy (GWh)
1	44.87	34.56	164847.135	1441.289	1.441
2	52.76	41.2	248199.255	2168.769	2.169
4	67.5	48.51	372894.585	3256.053	3.256
5	98.12	67.21	823396.129	7197.113	7.197
6	67.44	46.71	301659.165	2637.268	2.637
7	30.45	54	159239.173	1391.235	1.391
6	75.01	37	230645.154	2014.114	2.014
7	88.12	67	478478.183	4181.421	4.181
8	78.98	54	368486.893	3218.352	3.218
9	98.34	55	490960.574	4290.651	4.291
10	102	34	327855.084	2863.192	2.863

4. DISUSSION

The Black Volta Basin hosts a total of 166 distinct sites, each possessing varying levels of installed power capacity. These sites are categorized based on their potential for hydropower generation, which are further divided into Small (> 50 MW), Medium (51-100 MW), Large (<101 MW), and Largest (192 MW) classifications. Upon closer analysis, it was determined that within the Black Volta Basin, there exist 31 potential sites capable of generating small-scale hydropower, each with a capacity of 50 MW. Additionally, there are 68 sites suitable for mini-hydro projects, with capacities ranging from 51 to 101 MW. Furthermore, the study identified 62 sites with the potential to support larger-scale hydropower installations exceeding 101 MW, while a smaller number of five sites were found to have the highest capacity of 192 MW.

The significance of these findings extends to both the Black Volta Basin and the entire country of Ghana. The identification of these 166 potential sites underscores a substantial opportunity for the harnessing of hydropower resources. These sites, categorized based on their installed capacity, suggest a range of possibilities for energy generation. The presence of 31 small capacity sites and 68 mini-hydro capacity sites indicates a favorable environment

for decentralized energy generation. This decentralized approach holds promise for promoting small-scale hydroelectric projects, facilitating the diversification of the energy mix, and effectively meeting the energy requirements of local communities. In essence, these findings have the potential to shape the energy landscape of the Black Volta Basin and contribute significantly to Ghana's broader energy goals.

Furthermore, the identification of 62 potential sites with capacities exceeding 101 MW and five sites with the highest installed capacity of 192 MW highlights the potential for larger-scale hydroelectric projects. These projects have the capacity to significantly contribute to the overall energy generation in Ghana and meet the increasing demand for electricity in the country. The findings underscore the significant hydropower potential in the Black Volta Basin, presenting opportunities for both small-scale and large-scale energy generation. Leveraging these resources effectively can contribute to Ghana's energy security, promote renewable energy development, and facilitate sustainable economic growth. However, it is crucial to consider environmental and social impacts, as well as ensure responsible and inclusive project development and management to maximize the benefits and minimize potential drawbacks associated with hydropower projects.

Several comprehensive studies conducted by various researchers, such as Singh et al. (2019), Haque et al. (2018), Shrestha and Murthy (2015), Zaman et al. (2018), Atta-Obeng et al. (2017), Sharma et al. (2019), Chong et al. (2018), Tavares et al. (2020), Li et al. (2019), Baishya and Baruah (2018), and Girma et al. (2021), have collectively demonstrated the efficacy of Geographic Information Systems (GIS) and remote sensing technology in the identification of potential sites for energy generation along river courses. These research findings substantiate the practical utility of GIS and remote sensing techniques for the purpose of locating small to medium-scale hydropower projects. By leveraging topographical data, land use information, and hydrological data, these methods enable a precise and accurate assessment of suitable sites that can harness energy from the flowing water, thereby validating their application in this context.

5. CONCLUSION

The implementation of small hydropower plants along the course of the Black Volta River has been established as a technically viable endeavor. This endeavor was notably facilitated by the utilization of Geographic Information System (GIS) tools, particularly ArcGIS, in conjunction with the SWAT model. These technological tools played a pivotal role and brought significant benefits to various aspects of the project's development. A standout advantage derived from the integration of these tools was the creation of a digitized map. This map contained intricate details pertaining to hydraulic features and land cover, a feat made achievable through the use of satellite imagery. The incorporation of such remote sensing data streamlined the mapping process, rendering it more accessible and user-friendly. This mechanization not only expedited the workflow but also led to a marked enhancement in efficiency, resulting in substantial time savings and notable reductions in project expenditures.

Over the span of two decades, an observable trend has emerged in the Black Volta Basin. This trend encompasses a gradual reduction in densely vegetated areas like close scrub and mixed forests. In contrast, the coverage of stable grasslands has exhibited consistency, and fluctuations in water body extents have been minor in nature. Throughout the analysis, a total of 166 sites within the Black Volta Basin were identified as having potential for hydropower development. These sites displayed varying capacities for installed power. The classification of these potential sites was based on their power generation capabilities: Small (capacity exceeding 50 MW), Medium (ranging from 51 to 100 MW), Large (below 101 MW), and the most substantial category, Largest (with an installed capacity of 192 MW).

The detailed assessment unveiled specific insights into the distribution of potential hydropower sites within the Black Volta Basin. Among these, 31 sites exhibited potential for small-scale hydropower generation, with a capacity of up to 50 MW. Furthermore, the analysis identified 68 sites suitable for mini-hydro development, encompassing capacities between 51 MW and 101 MW. Additionally, a total of 62 sites demonstrated the potential for installations surpassing 101 MW in capacity. At the upper echelon, a select five sites showcased the highest conceivable installed capacity of 192 MW.

In conclusion, the successful establishment of small hydropower plants along the Black Volta River was achieved through the adept utilization of advanced GIS tools, particularly ArcGIS, and the application of the SWAT model. These technologies substantially facilitated the project's progress, enabling the creation of detailed digital maps and enhancing overall efficiency. The study's findings shed light on the evolving landscape of the Black Volta Basin and pinpointed numerous potential sites for hydropower development, varying in scale and capacity.

Conflict of Interest
The author(s) declare that they have no conflict of interest.

Funding
The author(s) received no financial support for the research, authorship, and/or publication of this article.

Data Availability
Data used for this research is available upon request from the corresponding author.

Notes
I appreciate the anonymous reviewer's comments, which I have noted and worked on to improve the manuscript's scholarly caliber and visibility.

REFERENCE

Allison, M.A., Nittrouer, C.A., Ogston, A.S., Mullarney, J.C., and Nguyen, T.T., 2017, Sedimentation and Survival of the Mekong Delta A Case Study of Decreased Sediment Supply and Accelerating Rates of Relative Sea Level Rise: Oceanography, v. 30, p. 98-109.

Anthony, E.J., Almar, R., and Aagaard, T., 2016, Recent shoreline changes in the Volta River delta, West Africa: the roles of natural processes and human impacts: African Journal of Aquatic Science, v. 41, p. 81-87.

Awotwi, A., Yeboah, F., and Kumi, M., 2015, Assessing the impact of land cover changes on water balance components of White Volta Basin in West Africa: Water and Environment Journal, v. 29, p. 259-267.

Barry, B., Obuobie, E., Andreini, M., Andah, W., and Pluquet, M., 2005, The Volta River Basin synthesis. Comparative study of river basin development and management. Comprehensive Assessment of Water Management in Agriculture: Colombo, Sri Lanka: International Water Management Institute (IWMI).

Bussi, G., Janes, V., Whitehead, P.G., Dadson, S.J., and Holman, I.P., 2017, Dynamic response of land use and river nutrient concentration to long-term climatic changes: Science of the Total Environment, v. 590, p. 818-831.

Crossman, J., Futter, M.N., Oni, S.K., Whitehead, P.G., Jin, L., Butterfield, D., Baulch, H.M., and Dillon, P.J., 2013, Impacts of climate change on hydrology and water quality: Future proofing management strategies in the Lake Simcoe watershed, Canada: Journal of Great Lakes Research, v. 39, p. 19-32.

Dickson, K.B., and Benneh, G., 1988, A new geography of Ghana: Longman Group UK Limited. Longman House, Burnt Mill, Harlow, Essex, England.

Ericson, J.P., Vorosmarty, C.J., Dingman, S.L., Ward, L.G., and Meybeck, M., 2006, Effective sea-level rise and deltas: Causes of change and human dimension implications: Global and Planetary Change, v. 50, p. 63-82.

Fang, G.H., Yang, J., Chen, Y.N., and Zammit, C., 2015, Comparing bias correction methods in downscaling meteorological variables for a hydrologic impact study in an arid area in China: Hydrol. Earth Syst. Sci., v. 19, p. 2547-2559.

Futter, M.N., Butterfield, D., Cosby, B.J., Dillon, P.J., Wade, A.J., and Whitehead, P.G., 2007, Modeling the mechanisms that control in-stream dissolved organic carbon dynamics in upland and forested catchments: Water Resources Research, v. 43, p. W02424, doi:10.1029/2006WR004960.

Gu, C.L., Hu, L.Q., Zhang, X.M., Wang, X.D., and Guo, J., 2011, Climate change and urbanization in the Yangtze River Delta: Habitat International, v. 35, p. 544-552.

Gyau-Boakye, P., and Tumbulto, J.W., 2000, The Volta Lake and Declining Rainfall and Streamflows in the Volta River Basin: Environment, Development and Sustainability, v. 2, p. 1-11.

Hill, C., Nicholls, R.J., Whitehead, P.W., Dunn, F., Haque, A., Appeaning Addo, K., and Raju, P.V., 2018, Delineating Climate Change Impacts on Biophysical Conditions in Populous Deltas Science of the Total Environment.

Hoang, L.P., Lauri, H., Kummu, M., Koponen, J., van Vliet, M.T.H., Supit, I., Leemans, R., Kabat, P., and Ludwig, F., 2016, Mekong River flow and hydrological extremes under climate change: Hydrology and Earth System Sciences, v. 20, p. 3027-3041.

IPCC, 2013a, Annex I: Atlas of Global and Regional Climate Projections: [van Oldenborgh, G.J., M. Collins, J. Arblaster, J.H. Christensen, J. Marotzke, S.B. Power, M. Rummukainen and T. Zhou (eds.)]. In: Climate Change 2013: The Physical Science Basis. Contribution of Working Group I to the Fifth Assessment Report of the Intergovernmental Panel on Climate Change [Stocker, T.F., D. Qin, G.-K. Plattner, M. Tignor, S.K. Allen, J. Boschung, A. Nauels, Y. Xia, V. Bex and P.M. Midgley (eds.)]. Cambridge University Press, Cambridge, United Kingdom and New York, NY, USA.

IPCC, 2013b, Summary for Policymakers. In: Climate Change 2013: The Physical Science Basis. Contribution of Working Group I to the Fifth Assessment Report of the Intergovernmental Panel on Climate Change: [Stocker, T.F., D. Qin, G.-K. Plattner, M. Tignor, S.K. Allen, J. Boschung, A. Nauels, Y. Xia, V. Bex and P.M. Midgley (eds.)]. Cambridge University Press, Cambridge, United Kingdom and New York, NY, USA.

IPCC, 2014, Summary for Policymakers. In: Climate Change 2014 Mitigation of Climate Change Working Group III Contribution to the Fifth Assessment Report of the Intergovernmental Panel on Climate Change: Cambridge, Cambridge Univ Press.

Jackson-Blake, L.A., Wade, A.J., Futter, M.N., Butterfield, D., Couture, R.M., Cox, B.A., Crossman, J., Ekholm, P., Halliday, S.J., Jin, L., Lawrence, D.S.L., Lepisto, A., Lin, Y., Rankinen, K., and Whitehead, P.G., 2016, The INtegrated CAtchment model of phosphorus dynamics (INCA-P): Description and demonstration of new model structure and equations: Environmental Modelling & Software, v. 83, p. 356-386.

Janes, T., McGrath, F., Macadam, I., and Jones, R., 2018, High-resolution climate projections for South Asia to inform climate impacts and adaptation studies in the Ganges-Brahmaputra-Meghna and Mahanadi deltas: Science of the Total Environment.

Jin, L., Whitehead, P., Siegel, D.I., and Findlay, S., 2011, Salting our landscape: An integrated catchment model using readily accessible data to assess emerging road salt contamination to streams: Environmental Pollution, v. 159, p. 1257-1265.

Jin, L., Whitehead, P.G., Baulch, H.M., Dillon, P.J., Butterfield, D., Oni, S.K., Futter, M.N., Crossman, J., and O'Connor, E.M., 2013, Modelling phosphorus in Lake Simcoe and its subcatchments: scenario analysis to assess alternative management strategies: Inland Waters, v. 3, p. 207-220.

Jin, L., Whitehead, P.G., Futter, M.N., and Lu, Z.L., 2012, Modelling the impacts of climate change on flow and nitrate in the River Thames: assessing potential adaptation strategies: Hydrology Research, v. 43, p. 902-916.

Kebede, A.S., Nicholls, R.J., Allan, A., Arto, I., Cazcarro, I., Fernandes, J.A., Hill, C.T., Hutton, C.W., Kay, S., Lazar, A.N., Macadam, I., Palmer, M., Suckall, N., Tompkins, E.L., Vincent, K., and Whitehead, P.G., 2018, Applying the Global RCP–SSP–SPA Scenario Framework at Sub-National Scale: A Multi-Scale and Participatory Scenario Approach: Science of the Total Environment, v. DECCMA Special Issue.

Lacombe, G., McCartney, M., and Forkuor, G., 2012, Drying climate in Ghana over the period 1960-2005: evidence from the resampling-based Mann-Kendall test at local and regional levels: Hydrological Sciences Journal-Journal Des Sciences Hydrologiques, v. 57, p. 1594-1609.

Lazar, A.N., Butterfield, D., Futter, M.N., Rankinen, K., Thouvenot-Korppoo, M., Jarritt, N., Lawrence, D.S.L., Wade, A.J., and Whitehead, P.G., 2010, An assessment of the fine sediment dynamics in an upland river system: INCA-Sed modifications and implications for fisheries: Science of the Total Environment, v. 408, p. 2555-2566.

Lu, Q., Whitehead, P.G., Bussi, G., Futter, M.N., and Nizzetto, L., 2017, Modelling metaldehyde in catchments: a River Thames case-study: Environmental Science-Processes & Impacts, v. 19, p. 586-595.

McCartney, M., Forkuor, G., Sood, A., Amisigo, B., Hattermann, F., and Muthuwatta, L., 2012, The water resource implications of changing climate in the Volta River Basin: Colombo, Sri Lanka: International Water Management Institute (IWMI). 40p. (IWMI Research Report 146). .

Mul, M., Obuobie, E., Appoh, R., Kankam-Yeboah, K., Bekoe-Obeng, E., Amisigo, B., Logah, F.Y., Ghansah, B., and McCartney, M., 2015, Water resources assessment of the Volta River Basin: Colombo, Sri Lanka: International Water Management Institute (IWMI). 78p. (IWMI Working Paper 166). doi: 10.5337/2015.220.

Nepal, S., and Shrestha, A.B., 2015, Impact of climate change on the hydrological regime of the Indus, Ganges and Brahmaputra river basins: a review of the literature: International Journal of Water Resources Development, v. 31, p. 201-218.

Nicholls, R.J., A.S., K., Allan, A., Arto, I., Cazcarro, I., Fernandes, J.A., Hill, C.T., Hutton, C.W., Kay, S., Lawn, J., Lázár, A.N., Macadam, I., Whitehead, P.G., and al, e., 2017, The DECCMA scenario framework: A multi-scale and participatory approach to explore the future migration and adaptation in deltas: DECCMA Working Paper, Deltas, Vulnerability and Climate Change: Migration and Adaptation, IDRC Project Number 107642. Available online at: www.deccma.com, date accessed

Nicholls, R.J., Hutton, C.W., Lazar, A.N., Allan, A., Adger, W.N., Adams, H., Wolf, J., Rahman, M., and Salehin, M., 2016, Integrated assessment of social and environmental sustainability dynamics in the Ganges-Brahmaputra-Meghna delta, Bangladesh: Estuarine Coastal and Shelf Science, v. 183, p. 370-381.

Oguntunde, P.G., 2004, Evapotranspiration and complementarity relations in the water balance of the Volta basin: Field measurements and GIS-based regional estimates: Ecology and Development Series No. 22. Göttingen, Germany: Cuvillier Verlag. 169p.

Owusu, K., Waylen, P., and Qiu, Y., 2008, Changing rainfall inputs in the Volta basin: implications for water sharing in Ghana: GeoJournal, v. 71, p. 201-210.

Pushpalatha, R., Perrin, C., Le Moine, N., and Andreassian, V., 2012, A review of efficiency criteria suitable for evaluating low-flow simulations: Journal of Hydrology, v. 420, p. 171-182.

Rankinen, K., Granlund, K., Futter, M.N., Butterfield, D., Wade, A.J., Skeffington, R., Arvola, L., Veijalainen, N., Huttunen, I., and Lepisto, A., 2013, Controls on inorganic nitrogen leaching from Finnish catchments assessed using a sensitivity and uncertainty analysis of the INCA-N model: Boreal Environment Research, v. 18, p. 373-386.

Wade, A.J., Butterfield, D., Lawrence, D.S., Bärlund, I., Ekholm, P., Lepistö, A., Yli-Halla, M., Rankinen, K., Granlund, K., Durand, P., and Kaste, Ø., 2009, The Integrated Catchment Model of Phosphorus (INCA-P), a new structure to simulate particulate and soluble phosphorus transport in European catchments, Deliverable 185 to the EU Euro-limpacs project, UCL, London, pp 67.

Wade, A.J., Durand, P., Beaujouan, V., Wessel, W.W., Raat, K.J., Whitehead, P.G., Butterfield, D., Rankinen, K., and Lepisto, A., 2002, A nitrogen model for European catchments: INCA, new model structure and equations: Hydrology and Earth System Sciences, v. 6, p. 559-582.

Whitehead, P.G., Barbour, E., Futter, M.N., Sarkar, S., Rodda, H., Caesar, J., Butterfield, D., Jin, L., Sinha, R., Nicholls, R., and Salehin, M., 2015a, Impacts of climate change and socio-economic scenarios on flow and water quality of the Ganges, Brahmaputra and Meghna (GBM) river systems: low flow and flood statistics: Environmental Science-Processes & Impacts, v. 17, p. 1057-1069.

Whitehead, P.G., Wilson, E.J., and Butterfield, D., 1998a, A semi-distributed Integrated Nitrogen model for multiple source assessment in Catchments (INCA): Part I - model structure and process equations: Science of the Total Environment, v. 210, p. 547-558.

Whitehead, P.G., Wilson, E.J., Butterfield, D., and Seed, K., 1998b, A semi-distributed integrated flow and nitrogen model for multiple source assessment in catchments (INCA): Part II - application to large river basins in south Wales and eastern England: Science of the Total Environment, v. 210, p. 559-583.